

Binding thermodynamics of host-guest systems with SMIRNOFF99Frosst 1.0.5 from the Open Force Field Initiative

This manuscript ([permalink](#)) was automatically generated from slochower/smirnoff-host-guest-manuscript@dfb7bc0 on May 23, 2019.

Authors

- **David R. Slochower**

 [0000-0003-3928-5050](#) ·  [slochower](#) ·  [drslochower](#)

Skaggs School of Pharmacy and Pharmaceutical Sciences, University of California, San Diego, La Jolla, CA 92093, USA

- **Niel M. Henriksen**

 [0000-0002-7916-0757](#) ·  [nhenriksen](#)

Atomwise, Inc., San Francisco, CA 94105, USA

- **Lee-Ping Wang**

 [0000-0003-3072-9946](#) ·  [leeping](#)

Department of Chemistry, University of California, Davis, CA 95616, USA

- **John D. Chodera**

 [0000-0003-0542-119X](#) ·  [jchodera](#) ·  [jchodera](#)

Computational and Systems Biology Program, Sloan Kettering Institute, Memorial Sloan Kettering Cancer Center, New York, NY 10065

- **David L. Mobley**

 [0000-0002-1083-5533](#) ·  [davidlmobley](#) ·  [davidlmobley](#)

Department of Pharmaceutical Sciences and Department of Chemistry, University of California, Irvine, CA 92697, USA

- **Michael K. Gilson**

 [0000-0002-3375-1738](#) ·  [michaelkgilson](#)

Skaggs School of Pharmacy and Pharmaceutical Sciences, University of California, San Diego, La Jolla, CA 92093, USA

Outstanding Issues

- [Update tables with CSV link and SMILES #42](#)
- [Update figure legends and labels with additional information #46](#)
- [Update GAFF v2.1 statistics in the text #47](#)
- [Consider adding discussion of Kendall's tau #49](#)
- [Update SI figure captions with letter numbering #50](#)
- [Refine language around "fewer parameters" claims #51](#)

Abstract

Designing ligands that bind their target biomolecules with high affinity and specificity is a key step in small-molecule drug discovery, but accurately predicting protein-ligand binding free energies remains challenging. Key sources of errors in the calculations include inadequate sampling of conformational space, ambiguous protonation states, and errors in force fields. Noncovalent complexes between a host molecule with a binding cavity and a drug-like guest molecules have emerged as powerful model systems for isolating the nature of errors in more complex protein-ligand binding systems, as their small size greatly facilitates conformational sampling, and one can choose systems that avoid ambiguities in protonation states. These features, combined with their ease of experimental characterization, make host-guest systems ideal model systems to test and ultimately optimize force fields in the context of binding calculations.

The Open Force Field Initiative aims to create a modern, open software infrastructure for automatically generating and validating force fields using high-quality data sets. The first force field to arise out of this effort, named SMIRNOFF99Frosst, has one tenth the number of parameters, in version 1.0.5, compared to typical general small molecule force fields, such as GAFF. Here, we evaluate the accuracy of this initial force field, using free energy calculations of 43 α and β -cyclodextrin host-guest pairs for which high-quality experimental thermodynamic data are available, and compare with matched calculations using two versions of GAFF. For all three force fields, we used TIP3P water and AM1-BCC charges. The calculations are performed using the attach-pull-release (APR) method as implemented in the open source package, PAPRIka. For binding free energies, the root mean square error of the SMIRNOFF99Frosst calculations relative to experiment is 0.9 kcal/mol, while the corresponding results for GAFF 1.7 and GAFF 2.1 are 0.9 kcal/mol and 1.7 kcal/mol, respectively, with 95% confidence ranges less than 0.4 kcal/mol for all three force fields. These results suggest that there is significant room for improvement in force fields and motivate further development of tools using host-guest binding data for the transparent and robust evaluation and optimization of future candidate parameter sets.

Introduction

The accurate prediction of protein-ligand binding free energies is a key goal of computational chemistry, with key applications in early stage drug discovery. However, calculations of protein-ligand binding thermodynamics still involve a number of challenging choices, including the choice of empirical force field, specifying the protonation states of ionizable residues, adding hydrogens and otherwise adjusting the initial protein structure, and positioning the candidate ligand in the binding pocket. Predictions of protein-ligand absolute binding free energies have achieved root mean square errors around 1-2 kcal/mol for “well-behaved” systems [1,2,3], with deviations an order of magnitude larger for some protein families with slow degrees of freedom [4]. Retrospective relative free energy calculations on a series of congeneric ligands, using proprietary methods, have also achieved root mean square errors compared to experiment of around 1 kcal/mol [5,6,7]. However, it is not possible to determine how much of the prediction error can be attributed to each of the decisions made by the modeler.

By minimizing the ambiguities involved in modeling protein-ligand complexes, host-guest systems offer a way to isolate and directly probe force field error. A variety of techniques for computing absolute binding free energies in host-guest systems have shown accuracy of ~1 kcal/mol, as highlighted in the recent SAMPL5 and SAMPL6 blind challenges [1,8]. These techniques include both quantum and classical dynamics, employing a range of energy and solvation models, with some techniques having knowledge-based steps, docking, or clustering [10,11,12,13,14,15,16,9]. The attach-pull-release (APR) method has consistently been ranked among the most reliable techniques for predicting binding thermodynamics of host-guest complexes in blind challenges [17,8]. In APR, the reversible work of transferring the guest from the binding site to solution, via a physical pathway, is computed using a series of umbrella sampling windows. Simulating each window and integrating over the partial derivative of the restraint energy with respect to the restraint target is used to generate a potential of mean force along the pulling coordinate,

yielding the binding free energy at standard state, ΔG° . Furthermore, subtracting the mean potential energies obtained from long simulations of the solvated bound complex and the solvated dissociated complex yields the binding enthalpy, ΔH . Together, ΔG° and ΔH can be combined to determine the binding entropy at standard state, ΔS° . Thus, APR provides the complete thermodynamic signature of a host-guest binding reaction: ΔG° , ΔH , and $-T\Delta S^\circ$.

Cyclodextrins, in particular, are ideal host molecules. They are neutral across the pH range, with well-characterized structures [18], and bind both small molecule fragments and drug-like guest molecules with reasonable affinity [19]. Moreover, cyclodextrins are stable in numerous conditions and their aqueous solubility allows a range of different experimental techniques to be used to measure their binding to guests [20]. Here, we report the calculation of binding free energies, enthalpies, and entropies of drug-like guest molecules to α - and β -cyclodextrin host molecules, converged to within ~ 0.1 kcal/mol, using the APR method. These calculations offer an opportunity to benchmark—and ultimately optimize—new and existing force fields. The first force field produced by the Open Force Field Initiative, SMIRNOFF99Frosst v1.0.5, was released in late 2018 [21, 22]. It is derived from AMBER parm99 [23] and Merck's parm@Frosst [24]. Instead of relying on atom types to assign force field parameters to compounds, which is the procedure followed by the leap program used to assign parameters to molecules in AmberTools [25], SMIRNOFF99Frosst and the Open Force Field Toolkit use separately defined local chemical environments for each atom, bond, angle, and dihedral, to apply force field parameters using SMIRKS strings [26]. This process simplifies and effectively uncouples the parameters for each term in the force field. For example, the addition of a new Lennard-Jones parameter does not require creating a new atom type that forces the addition of new bonded, angle, and dihedral parameters. This approach leads to a much leaner force field specification; there are over 3000 lines of parameters in GAFF v1.7 [27], over 6000 lines of parameters in GAFF v2.1, and just 322 lines of parameters in SMIRNOFF99Frosst version 1.0.5 [28]. It is important to note that SMIRNOFF99Frosst is not yet optimized at this stage, only compressed; subsequent work will focus on optimizing SMIRNOFF99Frosst and other SMIRNOFF-family force fields to fit quantum and experimental data [29]. In the following text, SMIRNOFF99Frosst refers to version 1.0.5 of the force field, unless otherwise noted.

Thus far, SMIRNOFF99Frosst has been tested on hydration free energies of 642 small molecules and the densities and dielectric constants of 45 pure organic liquids [21]. Here, we benchmark SMIRNOFF99Frosst, GAFF v1.7, and GAFF v2.1 using noncovalent binding thermodynamics for two flexible host molecules and thirty three guests containing three different functional group moieties. We first compare the results of SMIRNOFF99Frosst with those of the conventional force fields GAFF v1.7 and GAFF v2.1, based on calculations of experimental binding free energies, enthalpies, and entropies. We then characterize the differences in host conformations sampled by SMIRNOFF99Frosst compared to the other two force fields.

Methods

Choice of host-guest systems

In this study, we report the binding thermodynamics of 43 host-guest complexes (Figure 1 and Table 1) computed using three different force fields. The complexes consist of either α - or β -cyclodextrin as host molecules and a series of small molecule guests containing ammonium, carboxylate, or cyclic alcohol functional groups. The cyclodextrins in the current study are cyclic polymers consisting of six (α CD) or seven (β CD) glucose monomers in the shape of a truncated cone. The equilibrium constants and standard molar enthalpies of binding for these 43 complexes have been measured using isothermal titration calorimetry (ITC) and nuclear magnetic resonance spectroscopy (NMR) [30]. Calculations on these host-guest systems have been performed previously [31], and, as in the prior study, we considered only a single stereoisomer for the 1-methylammonium guests because it was not clear whether a mixture or a pure solution was used in Rekharsky, et al. [30], and the ΔG difference between each stereoisomer is expected to be < 0.1 kcal/mol [32].

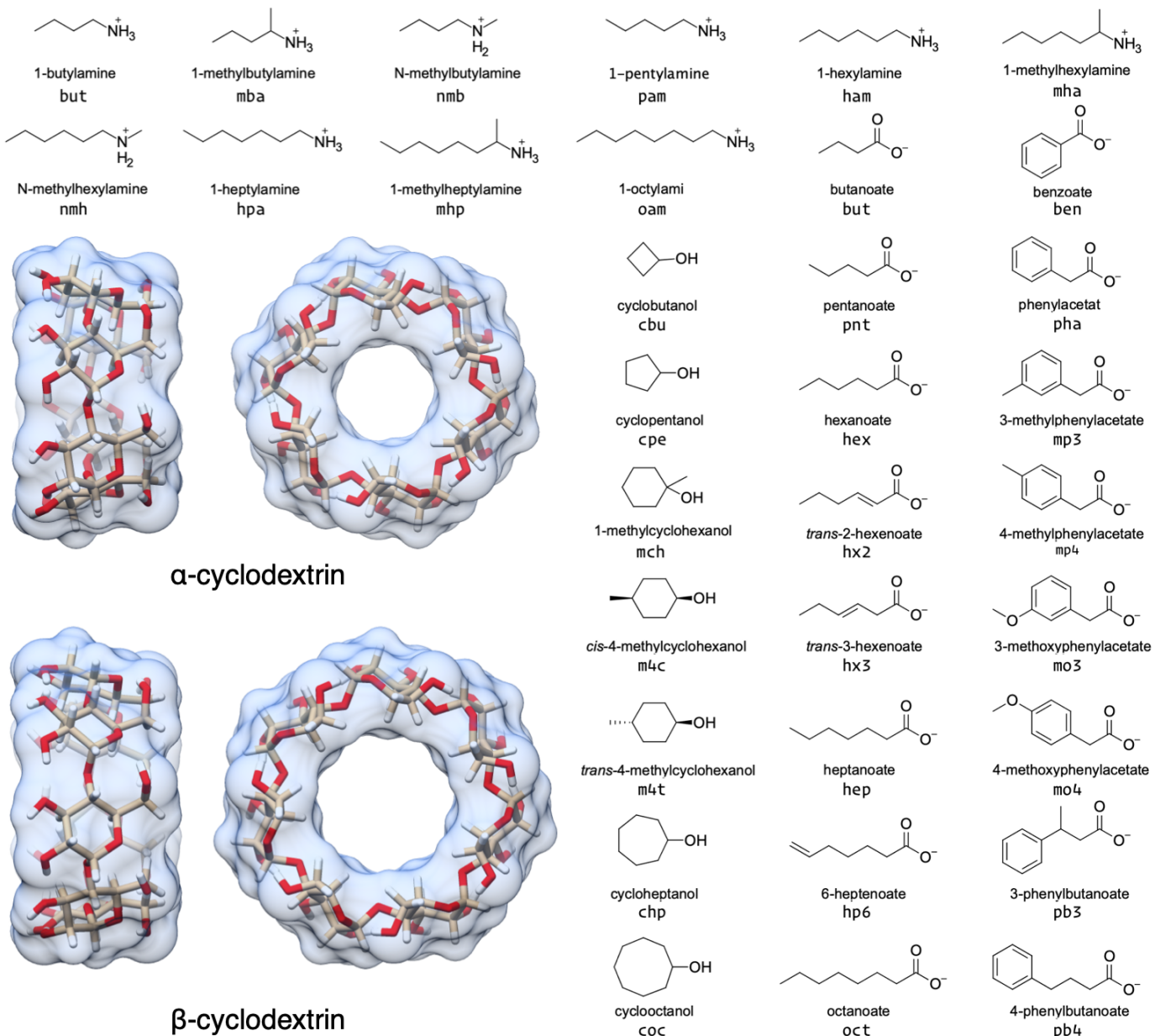


Figure 1: Structures of the two cyclodextrin hosts and 33 guest molecules in this study which together comprise 43 unique host-guest pairs.

Table 1: The 43 unique host-guest combinations used in this study. The formal charge of each guest is listed in brackets. The guest names correspond to Tables 1 and 2 in Rekharsky et al. [30]. ^a Only the R enantiomer was considered. ^b Only the S enantiomer was considered.

Host-guest ID	Host	Guest	Charge
a-bam	αCD	1-butylamine	+1
a-nmb	αCD	n-methylbutylamine	+1
a-mba	αCD	1-methylbutylamine ^a	+1
a-pam	αCD	1-pentylamine	+1
a-ham	αCD	1-hexylamine	+1
a-nmh	αCD	n-methylhexylamine	+1
a-mha	αCD	1-methylhexylamine ^a	+1
a-hpa	αCD	1-heptylamine	+1
a-mhp	αCD	1-methylheptylamine ^b	+1
a-oam	αCD	1-octylamine	+1

Host-guest ID	Host	Guest	Charge
b-ham	β CD	1-hexylamine	+1
b-mha	β CD	1-methylhexylamine ^a	+1
b-oam	β CD	1-octylamine	+1
a-cbu	α CD	cyclobutanol	0
a-cpe	α CD	cyclopentanol	0
a-chp	α CD	cycloheptanol	0
a-coc	α CD	cyclooctanol	0
b-cbu	β CD	cyclobutanol	0
b-cpe	β CD	cyclopentanol	0
b-mch	β CD	1-methylcyclohexanol	0
b-m4c	β CD	cis-4-methylcyclohexanol	0
b-m4t	β CD	trans-4-methylcyclohexanol	0
b-chp	β CD	cycloheptanol	0
b-coc	β CD	cyclooctanol	0
a-but	α CD	butanoate	-1
a-pnt	α CD	pentanoate	-1
a-hex	α CD	hexanoate	-1
a-hx2	α CD	trans-2-hexenoate	-1
a-hx3	α CD	trans-3-hexenoate	-1
a-hep	α CD	heptanoate	-1
a-hp6	α CD	6-heptenoate	-1
a-oct	α CD	octanoate	-1
b-pnt	β CD	pentanoate	-1
b-hex	β CD	hexanoate	-1
b-hep	β CD	heptanoate	-1
b-ben	β CD	benzoate	-1
b-pha	β CD	phenylacetate	-1
b-mp3	β CD	3-methylphenylacetate	-1
b-mp4	β CD	4-methylphenylacetate	-1
b-mo3	β CD	3-methoxyphenylacetate	-1
b-mo4	β CD	4-methoxyphenylacetate	-1
b-pb3	β CD	3-phenylbutanoate	-1
b-pb4	β CD	4-phenylbutanoate	-1

Application of force field parameters

We sought to compare force fields directly, and as such, attempted to minimize additional differences between the simulations with each force field. In all simulations, we applied AM1-BCC [33,34] partial atomic charges to both the host and guest molecules using the antechamber program. The host charges were calculated using a single glucose molecule with methoxy caps on the O1 and O4 alcohols (Figure 2); each glucose monomer in the cyclodextrin polymer has identical charges. After removing the capping

atoms, the remaining charges were adjusted in small increments to ensure neutrality of the glucose molecule. Using the entire α CD molecule as an input to `antechamber` results in partial atomic charges that differ by ± 0.02 e, compared to using a single monomer, and requires reducing the maximum path length used to determine the equivalence of atomic charges (Figure 16). We used TIP3P water [35] and Joung-Cheatham monovalent ion parameters [36] in each simulation set.

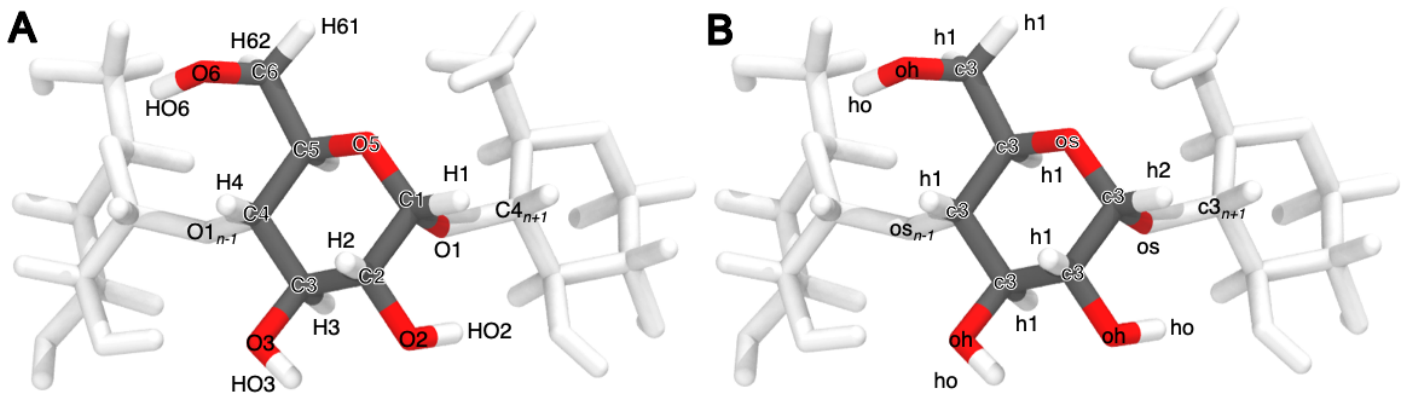


Figure 2: Atom names (A) and GAFF atom types (B) for a glucose monomer in α CD shown with two flanking monomers. The remaining three glucose monomers are hidden for clarity.

GAFF v1.7 bond, angle, torsion, and Lennard-Jones parameters were applied using the `t leap` program distributed with AmberTools16. GAFF v2.1 parameters were applied in an identical manner to the GAFF v1.7 parameters, using the `t leap` program distributed with AmberTools18 and substituting `leaprc.gaff` for `leaprc.gaff2` in the `t leap` input file.

To apply SMIRNOFF99Frosst parameters, we followed a [multistep process](#), beginning with the AMBER-format `.prmtop` and `.inpcrd` GAFF v1.7 files. The host and guest molecules were parameterized with version 0.0.3 of the Open Force Field Toolkit, which reads molecular coordinates and topologies and creates a serialized representation of the molecular system, version 1.0.5 of the SMIRNOFF99Frosst force field, specified in version 1.0 of the SMIRNOFF format. Once parameterized with SMIRNOFF99Frosst, the topology and coordinates for the host-guest complex were combined with the solvent and ions, which retained their TIP3P water parameters and Joung-Cheatham ion parameters, respectively. This was accomplished by the `ParmEd` program [37], which enables saving the OpenMM system created by the Open Force Field Toolkit in AMBER-format `.prmtop` and `.inpcrd` files.

Thermodynamic calculation

We used the attach-pull-release (APR) method, as implemented in the open source package pAPRika version 0.0.3, to calculate absolute binding free energies. A complete description of the APR method has been provided in the literature [13, 17, 38, 39]. The attachment and release phases consisted of 15 independent windows. During the attachment phase, the force constants on the host and guest are scaled by a λ parameter that goes from $\lambda = 0$, at which point all restraints are turned off, to $\lambda = 1$, at which point all restraints are at their maximum force constant. The λ windows are more densely spaced where the force constant is smaller to improve sampling along highly curved regions of the potential of mean force. Conformational restraints were applied between neighboring glucose units of the cyclodextrin to minimize deformations of the host molecule as the guest molecule is pulled out. These restraints were applied along the pseudodihedrals $O_{5n}-C_{1n}-O_{1n}-C_{4n+1}$ and $C_{1n}-O_{1n}-C_{4n+1}-C_{5n+1}$ to improve convergence and sampling of the bound state (Figure 2 for atom names). To further improve sampling of weak-binding guests, we applied a hard wall restraint that confined the guest molecule to within a sphere of 12.3 and 13.5 Å of α CD and β CD, respectively, during the bound state. The release phase is the conceptual reverse of the attach phase, in which the conformational restraints on the host are gradually turned off ($\lambda = 1 \rightarrow 0$) in the absence of the guest. This explicit release phase is performed once for α CD and once for β CD, as it is independent of guest molecule. Finally, an analytic correction is performed to

compute the work of moving the guest from the restricted volume enforced by the APR restraints to standard state at 1 M concentration.

The pulling phase consisted of 45 independent, equally spaced windows. During the pulling phase, the λ parameter represents the target value of a distance restraint with constant force constant. This target distance is increased uniformly in 45 increments of 0.4 Å, yielding windows that separate the host and guest by 18 Å over the course of the calculation.

Due to the asymmetry of the primary and secondary alcohols of cyclodextrin (Figure 18), and the lack of symmetry of the small molecule guests, there are generally two distinct binding poses that do not interconvert during the simulation timescale. To account for this effect, we separately compute the binding free energy and enthalpy for each orientation [13] and combine the results to produce a single value for each host-guest combination using the following equation:

$$\Delta G^\circ = -RT \ln(\exp(-\beta\Delta G_{\text{primary}}^\circ) + \exp(-\beta\Delta G_{\text{secondary}}^\circ)).$$

The total binding enthalpy is weighted by both the binding enthalpy and binding free energy in each orientation using the following equation:

$$\Delta H = \frac{\Delta H_{\text{primary}} \exp(-\beta\Delta G_{\text{primary}}^\circ) + \Delta H_{\text{secondary}} \exp(-\beta\Delta G_{\text{secondary}}^\circ)}{\exp(-\beta\Delta G_{\text{primary}}^\circ) + \exp(-\beta\Delta G_{\text{secondary}}^\circ)}.$$

In this manuscript, we refer to calculations where the guest is pulled out of the primary face of cyclodextrin with a `-p` suffix and calculations whereby the guest is pulled out of the secondary orientation with a `-s` suffix.

Thermodynamic integration was used to compute the binding free energy (ΔG°). The binding enthalpy (ΔH) was computed as the difference in mean potential energy of the bound state (in the absence of any restraints) and the unbound state (where the guest is held far away from the host, but the conformational restraints on the host are disabled). The binding entropy (ΔS°) was computed by subtraction using ΔG° and ΔH .

Simulations

Simulations were performed with the `pmemd.cuda` module of AMBER 16 (calculations with the GAFF v1.7 force field) and AMBER 18 (calculations with the GAFF v2.1 and SMIRNOFF99Frosst force fields) molecular dynamics software [25,40]. Each window for each system was independently solvated and simulated. The host-guest simulations using GAFF v1.7 were previously published in Henriksen, et al. [31] and are described in additional detail therein. Solvation consisted of 2000 TIP3P waters for the αCD systems and 2210 waters for the βCD systems in an orthorhombic box. The host and guest were oriented via non-interacting dummy atoms along the simulation box's long z axis, to allow use of an elongated periodic box that reduces the amount of solvent required for the calculation. Each simulation contained enough Na^+ or Cl^- ions to neutralize the host-guest complex and an additional 50 mM NaCl to match the experimental conditions in [30]. In the GAFF simulations, hydrogen mass repartitioning [41] was used to adjust the mass of hydrogen by a factor of 3, keeping the total molecular weight of each molecule constant and enabling a simulation timestep of 4 fs. Hydrogen mass repartitioning produces excellent agreement on thermodynamic observables for other cyclodextrin-guest calculations, with deviations of 0.05 kcal/mol on ΔG° and 0.1 kcal/mol on ΔH [13]. Equilibration consisted of 50,000 steps of energy minimization, 100 ps of heating from 0 to 300 K, and then 2000 ps of additional NPT simulation. A Langevin thermostat, the Monte Carlo barostat, a nonbonded cutoff of 9 Å and default PME parameters, were used for the NPT simulations. An isotropic analytic correction to the Lennard-Jones interactions is applied beyond the cutoff distance [42]. Production NPT simulations were run for a minimum of 2.5 ns and maximum of 50 ns per window, except

for the windows used to calculate the enthalpy, which were each simulated for 1 μ s. In the GAFF v1.7 and GAFF v2.1 simulations, the exact length of each window's simulation was determined by the uncertainty in the work done in each λ window. In particular, for restraint energy U in λ window i , each window (except for the windows used to calculate ΔH) was simulated until the value of $w(\lambda_i)$, defined as

$$w(\lambda_i) = \begin{cases} \left(\frac{\partial U}{\partial \lambda_i} \right)_{\text{SEM}} \frac{\lambda_{i+1}}{2} & i = 0 \\ \left(\frac{\partial U}{\partial \lambda_i} \right)_{\text{SEM}} \frac{\lambda_{i+1} - \lambda_{i-1}}{2} & i \in [1, N-1] \\ \left(\frac{\partial U}{\partial \lambda_i} \right)_{\text{SEM}} \frac{1 - \lambda_{i-1}}{2} & i = N \end{cases} \quad (1)$$

fell below a threshold of 0.02 kcal/mol during the attach phase and 0.1 kcal/mol during the pull phase. The second term in Equation 1 scales the uncertainty in the work in each λ window by the nonuniform spacing of the λ windows. Excluding the first and last window, the average window length was 11.8 ns and 5.39 ns for GAFF v1.7 and GAFF v2.1 simulations, respectively. We took a more direct approach with the SMIRNOFF99Frosst simulations, targeting uncertainties of the same magnitude as in the GAFF simulations, by running each window for a constant length of 10 ns, except for the first and last window which ran for 1 μ s to converge ΔH .

Statistics

The uncertainty in the work done by each restraint in each simulation window, $\left(\frac{\partial U}{\partial \lambda_i} \right)_{\text{SEM}}$, was estimated using blocking analysis [43], in a manner which has been shown to yield good agreement with uncertainties obtained from independent replicates [13]. In particular, rather than looking for a plateau in the SEM as the size of the blocks increased, as originally described by Flyvbjerg and Petersen [43], we instead use the largest standard error of the mean (SEM) obtained for any block size. This avoids the requirement of detecting a plateau and yields a more conservative estimate; i.e., a larger SEM. Then, using Gaussians with the mean and SEM of $\frac{\partial U}{\partial \lambda}$ in each window, new values of $\frac{\partial U}{\partial \lambda}$ were bootstrap sampled for each window 100,000 times and combined to create artificial data for 100,000 notional APR calculations. These were integrated across all windows with splines to generate 100,000 estimates of ΔG° . We report the mean and standard deviation of these 100,000 results as the final mean and its SEM. The SEM of ΔH was computed from the SEM of the total potential energy in each end point window, estimated using blocking analysis, added in quadrature. The standard error of the mean of $-T\Delta S^\circ$ was calculated using the uncertainties in ΔG° and ΔH added in quadrature.

For each force field, we computed the root mean squared error (RMSE), mean signed error (MSE), the coefficient of determination (R^2), Kendall's rank correlation coefficient (τ), and the slope and intercept of the linear regressions of the computed properties against the experimental values. The R^2 values for the subsets of ligand with each are also reported in the bottom right corner in each graph. Comparisons with experiment have 43 measurements, for the 43 unique host-guest complexes listed in Table 1; comparisons between force fields have 86 data points, representing the calculations for the two orientations of the guest, "p" and "s", in the binding site (see above). The overall RMSE and R^2 statistics for each comparison are reported as the sample mean estimated from using all the data, with the 95% confidence interval, from bootstrapping, in brackets.

Results

This results section is organized as follows. We first present a comparison of SMIRNOFF99Frosst and two iterations of the General AMBER Force Field (GAFF [27]) on predicting binding free energies (ΔG) and

binding enthalpies (ΔH) of small molecule guests to α -cyclodextrin (α CD) and β -cyclodextrin (β CD). We then detail how the conformational preferences of guest molecules changes between force fields and finally we summarize the parameter differences between SMIRNOFF99Frosst and GAFF along with the effects of the parameter differences.

Comparison with experimental binding free energies, enthalpies, and entropies

Binding free energies

Despite having far fewer numerical parameters, SMIRNOFF99Frosst does about as well as GAFF v1.7 and better than GAFF v2.1 on predicting ΔG compared to values measured using ITC or NMR.

SMIRNOFF99Frosst has an overall deviation from experiment of 0.91 kcal/mol, 95% CI [0.71, 1.13] on binding free energies across the 43 host-guest systems, compared to 0.88 kcal/mol, 95% CI [0.71, 1.08] for GAFF v1.7 and 1.68 kcal/mol, 95% CI [1.51, 1.85] for GAFF v2.1 (Figures 3, 17, Table 2, Table 5, Table 6, and Table 7) On the whole, GAFF v1.7 agrees well with SMIRNOFF99Frosst (Figure 21); the overall root mean squared error (RMSE) and mean signed error (MSE) between the methods is 0.80 kcal/mol, 95% CI [0.58, 1.04] and -0.47 kcal/mol, 95% CI [-0.67, -0.28], respectively. Both SMIRNOFF99Frosst and GAFF v1.7 systematically underestimate the ΔG for cyclic alcohols. GAFF v2.1 significantly overestimates the binding of all compounds by more than 1.5 kcal/mol, with a mean signed error of -1.56 kcal/mol, 95% CI [-1.74, -1.37]. Despite this, GAFF v2.1 has a strikingly strong correlation with experiment across all functional group classes. This may be traced to differences in host conformations sampled by GAFF v2.1, which indicate a more consistently open cyclodextrin “pocket” for guests to bind (Figure 14).

Binding enthalpies and entropies

On both binding enthalpies and entropies, SMIRNOFF99Frosst and GAFF v1.7 agree reasonably well with each other (ΔH RMSE = 1.65 kcal/mol, 95% CI [1.32, 2.02], $-T\Delta S$ RMSE = 1.59 kcal/mol, 95% CI [1.24, 1.96]) (Figure 21). The deviations between SMIRNOFF99Frosst and GAFF v2.1 are higher for ΔH (RMSE = 2.96 kcal/mol, 95% CI [2.52, 3.42]) and lower for $-T\Delta S$ (RMSE = 1.55 kcal/mol, 95% CI [1.25, 1.85]) On binding enthalpies, SMIRNOFF99Frosst agrees the best with experiment (RMSE = 1.85 kcal/mol, 95% CI [1.40, 2.29]), followed by GAFF v2.1 (RMSE = 2.21 kcal/mol, 95% CI [1.77, 2.66]), and then GAFF v1.7 (RMSE = 2.54 kcal/mol, 95% CI [2.08, 2.99]), In some cases, GAFF v1.7 underestimates ΔH by over 3 kcal/mol and up to 5 kcal/mol (b-chp).

On binding entropies, GAFF v2.1 has the lowest RMSE compared to experiment (RMSE = 1.47 kcal/mol, 95% CI [1.09, 1.99]), followed by SMIRNOFF99Frosst (RMSE = 1.90 kcal/mol, 95% CI [1.49, 2.32]), and GAFF v1.7 (RMSE = 2.21 kcal/mol, 95% CI [1.74, 2.68]) (Figure 17).

All force fields perform poorly predicting $-T\Delta S$ for carboxylate guests. It is worth noting that all force fields predict a much smaller entropic component of binding for a-coc by 3-5 kcal/mol, which does not easily fit inside the primary cavity of cyclodextrin (Figure 4).



Figure 3: Comparison of calculated absolute binding free energies (ΔG) and binding enthalpies (ΔH) with experiment with SMIRNOFF99Frosst parameters (A, B), GAFF v1.7 parameters (C, D), or GAFF v2.1 parameters (E, F) applied to both host and guest. The orange, blue, and purple coloring distinguish the functional group of the guest as an ammonium, alcohol, or carboxylate, respectively.

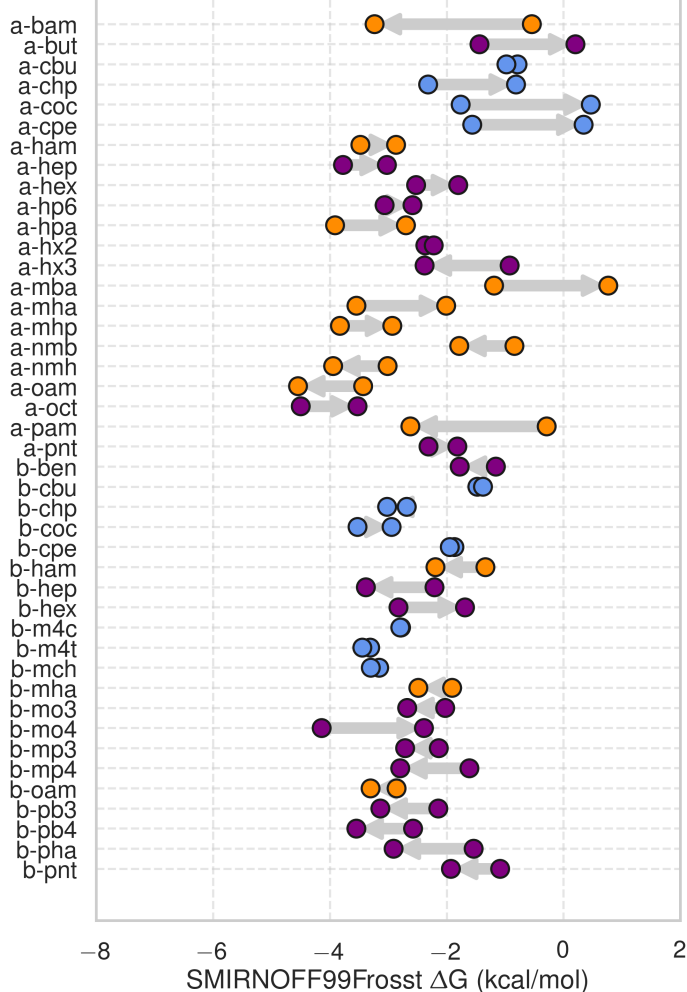
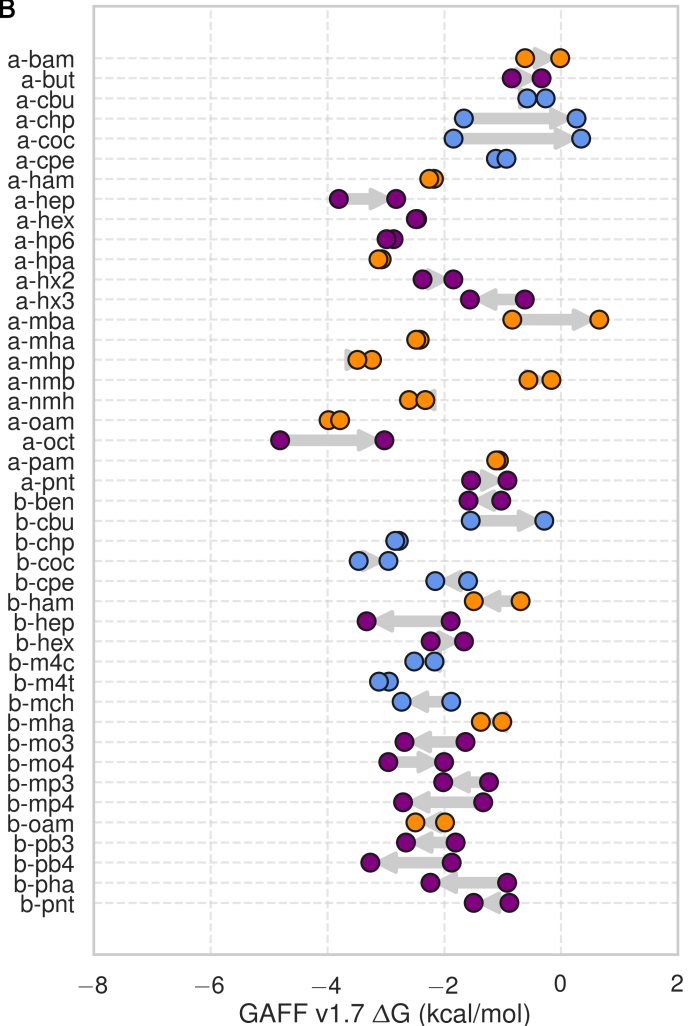
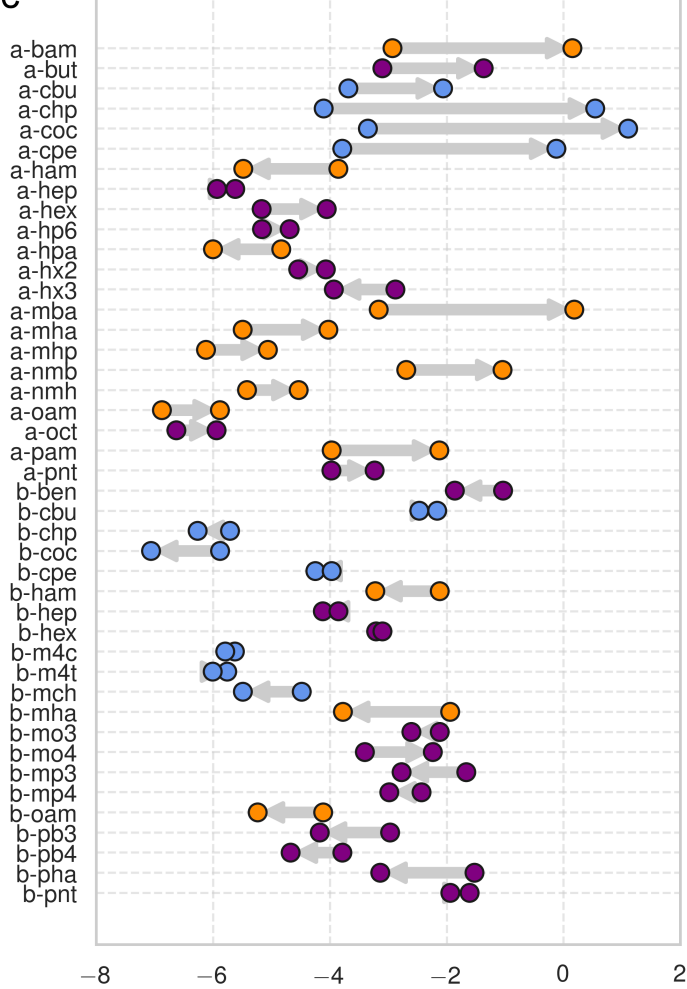
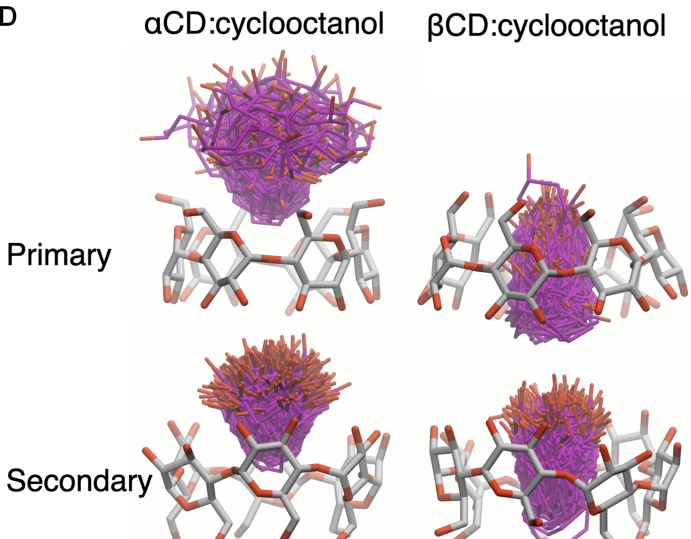
Table 2: Predicted thermodynamic properties for each force field relative to experiment.

		RMSE		MSE		R ²		Slope		Intercept	
ΔG	SMIRNOFF99Frosst	0.91	[0.71, 1.13]	-0.01	[-0.29, 0.26]	0.34	[0.12, 0.56]	0.49	[0.26, 0.72]	-1.55	[-0.80, -2.29]
ΔG	GAFF v1.7	0.88	[0.71, 1.08]	0.46	[0.23, 0.69]	0.54	[0.33, 0.71]	0.69	[0.47, 0.91]	-0.47	[0.22, -1.16]
ΔG	GAFF v2.1	1.68	[1.51, 1.85]	-1.56	[-1.74, -1.37]	0.82	[0.61, 0.92]	1.19	[0.96, 1.34]	-1.00	[-0.52, -1.62]
ΔH	SMIRNOFF99Frosst	1.85	[1.40, 2.30]	0.77	[0.26, 1.28]	0.44	[0.21, 0.66]	0.85	[0.54, 1.19]	0.41	[1.55, -0.50]
ΔH	GAFF v1.7	2.54	[2.08, 2.99]	1.84	[1.31, 2.37]	0.39	[0.17, 0.62]	0.80	[0.47, 1.18]	1.36	[2.66, 0.31]
ΔH	GAFF v2.1	2.21	[1.77, 2.66]	-1.64	[-2.10, -1.20]	0.75	[0.57, 0.87]	1.38	[1.15, 1.63]	-0.69	[0.15, -1.43]
$-\Delta S$	SMIRNOFF99Frosst	1.90	[1.49, 2.32]	-0.78	[-1.29, -0.25]	0.40	[0.14, 0.63]	0.90	[0.51, 1.29]	-0.83	[-0.34, -1.34]
$-\Delta S$	GAFF v1.7	2.21	[1.74, 2.68]	-1.38	[-1.90, -0.85]	0.43	[0.16, 0.68]	0.95	[0.54, 1.38]	-1.41	[-0.95, -1.89]
$-\Delta S$	GAFF v2.1	1.47	[1.09, 2.00]	0.08	[-0.35, 0.54]	0.60	[0.29, 0.80]	1.14	[0.75, 1.47]	0.15	[0.57, -0.27]

Guest preferences for binding in the primary or secondary cyclodextrin cavity

The asymmetry of the hosts and the guests leads to two distinct bound states for each host-guest pair: one where the primary functional group of the guest interacts with the primary alcohols of the host and a second conformation where the primary functional group of the guest interacts with the secondary alcohols (18).

The difference in binding free energy between either orientation ($\Delta\Delta G_{\text{orientation}}$) can be large, around ~ 2 kcal/mol for SMIRNOFF99Frosst and GAFF v1.7 and ~ 5 kcal/mol for GAFF v2.1. SMIRNOFF99Frosst predicts the largest $\Delta\Delta G_{\text{orientation}}$ for the ammonium-containing butylamine and pentylamine with α CD (4), with the primary orientation being more favorable. GAFF v1.7 predicts a large $\Delta\Delta G_{\text{orientation}}$ for the cyclic alcohols cyclooctanol and cycloheptanol, with the secondary orientation having a more favorable ΔG . This effect is even more apparent with GAFF v2.1 where the $\Delta\Delta G_{\text{orientation}}$ for a-chp and a-coc is greater than 4 kcal/mol. This effect is due, at least in part, to sampling challenges in the bound state for very large guests (Figure 4, D), especially in the narrow primary cavity of the smaller α -cyclodextrin.

A**B****C****D**

GAFF v2.1 ΔG (kcal/mol)

Figure 4: The differences in binding free energy (ΔG) between guests in either the primary or secondary orientation of α CD or β CD, for SMIRNOFF99Frosst (A), GAFF v1.7 (B), or GAFF v2.1 (C). Arrows point from ΔG for the secondary to ΔG for the primary cavity. (D) An overlay of cyclooctanol bound state positions (400 snapshots over 1 μ s) with α CD in GAFF v2.1.

Guest preferences for α CD and β CD

Ten guests in the data set bind both α CD and β CD. These ten guests show different patterns of binding between the two host molecules. For example, SMIRNOFF99Frosst underestimates the binding free energy of cyclooctanol both orientations by the same amount (Figure 5). However, despite underestimating the binding free energy of cyclobutanol for α CD by ~ 0.7 kcal/mol, the binding affinity prediction for β CD is very slightly overestimated by ~ 0.3 kcal/mol (Table 5). Very similar patterns are observed for GAFF v1.7 and both force fields appear to perform better overall on binding affinities to α CD compared to β CD (Figure 24).

As is the case with the difference in binding free energy between guest orientations, the difference in binding free energy between host molecules using GAFF v2.1 is large. There does not appear to be a clear difference in the accuracy of the predictions for α CD versus β CD (Figure 24).

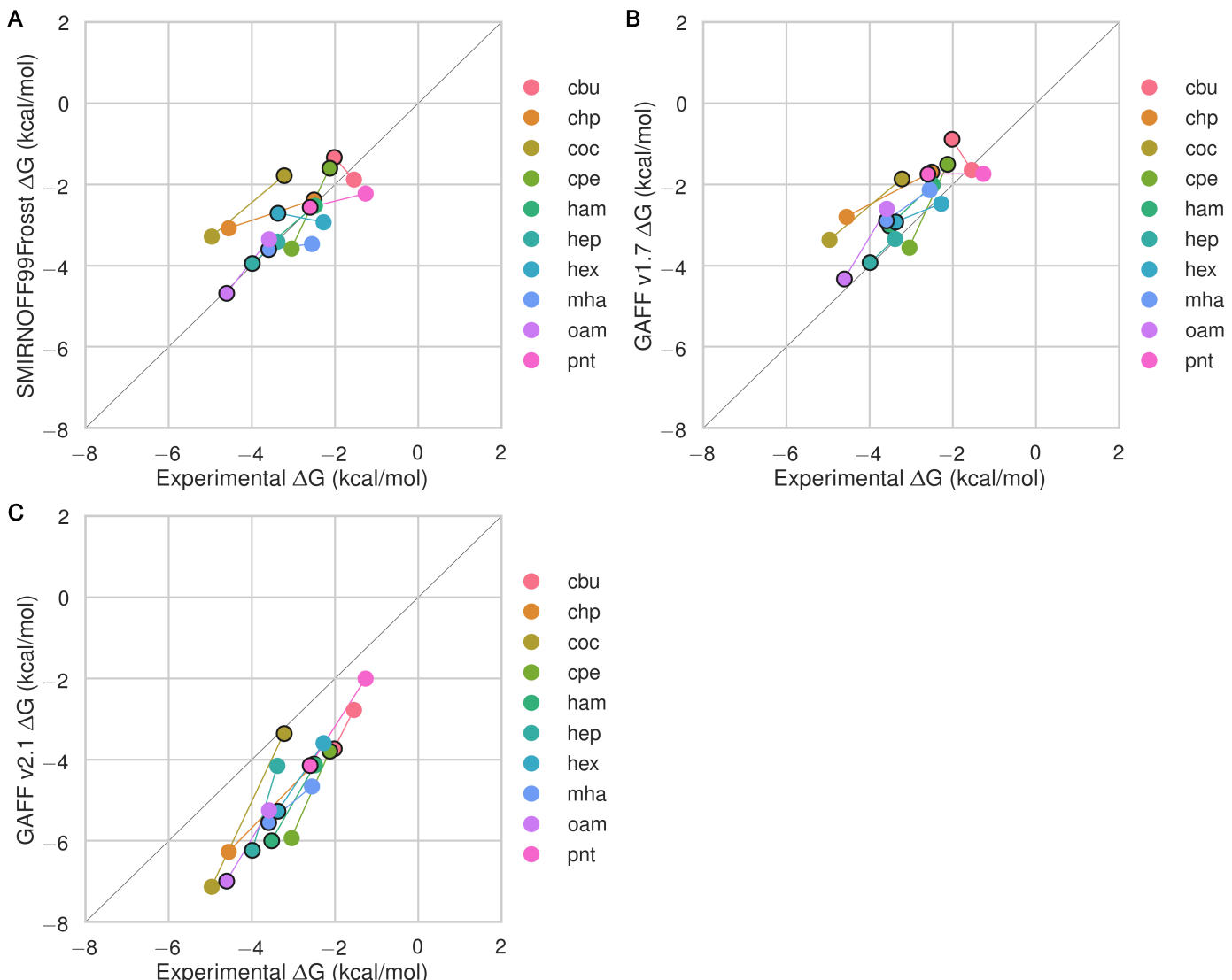


Figure 5: Shown are the α CD and β CD binding free energies for each guest, highlighting the differences in binding to the two hosts for SMIRNOFF99Frosst (A), GAFF v1.7 (B), or GAFF v2.1 (C). The binding affinity for α CD is circled in black. Thin colored lines connect data points for the same guest. Color is used purely to distinguish among the guests.

Trends by guest functional group

SMIRNOFF99Frosst does a good job ($\text{MSE} = -0.10 \text{ kcal/mol}$, 95% CI [-0.54, 0.30] and $\text{RMSE} = 0.76 \text{ kcal/mol}$, 95% CI [0.43, 1.12]) estimating the binding free energy of ammonium-containing guests to both αCD and βCD (Figure 6 and Table 8). Shorter chain molecules bind less strongly and the same guest binds more strongly to αCD than βCD .

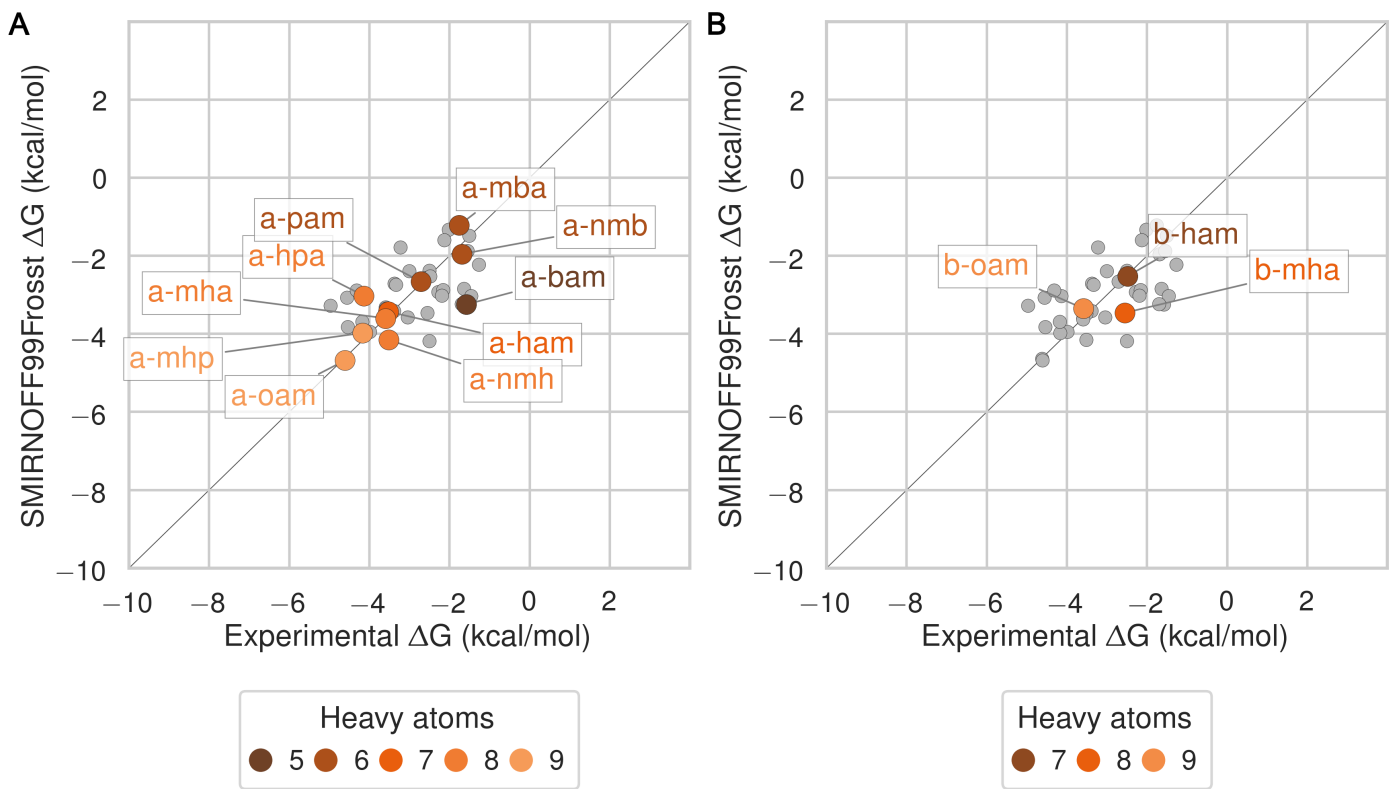


Figure 6: Binding free energy (ΔG) comparisons showing ammonium guests in color and highlighted, for αCD (A) and βCD (B). Darker colors indicate shorter chain molecules. Non-highlighted guests are shown as smaller gray circles.

SMIRNOFF99Frosst performs reasonably on cyclic alcohols ($\text{MSE} = 0.70 \text{ kcal/mol}$, 95% CI [0.22, 1.21] and $\text{RMSE} = 1.07 \text{ kcal/mol}$, 95% CI [0.66, 1.58]) (Figure 7 and Table 10). The predictions for αCD are uniformly underpredicted while those for βCD are mostly under-predicted. The predicted ΔG for cyclooctanol with αCD is particularly poor due to a poor fit in the bound state (Figure 4). The experimental uncertainty assigned to cyclooctanol is also much higher than the uncertainty of other guest compounds, due to an uncertainty in its concentration that can likely trace to its poor solubility at the experimental conditions ([30], tables 1 and 2).



Figure 7: Binding free energy (ΔG) comparisons showing alcohols guests in color and highlighted, for α CD (A) and β CD (B). Darker colors indicate smaller molecules. Non-highlighted guests are shown as smaller gray circles.

The binding affinity of carboxylate guests to both α CD and β CD is well characterized by SMIRNOFF99Frosst (MSE = -0.36 kcal/mol, 95% CI [-0.73, -0.01] and RMSE = 0.87 kcal/mol, 95% CI [0.58, 1.16]) (Figure 8 and Table 9).

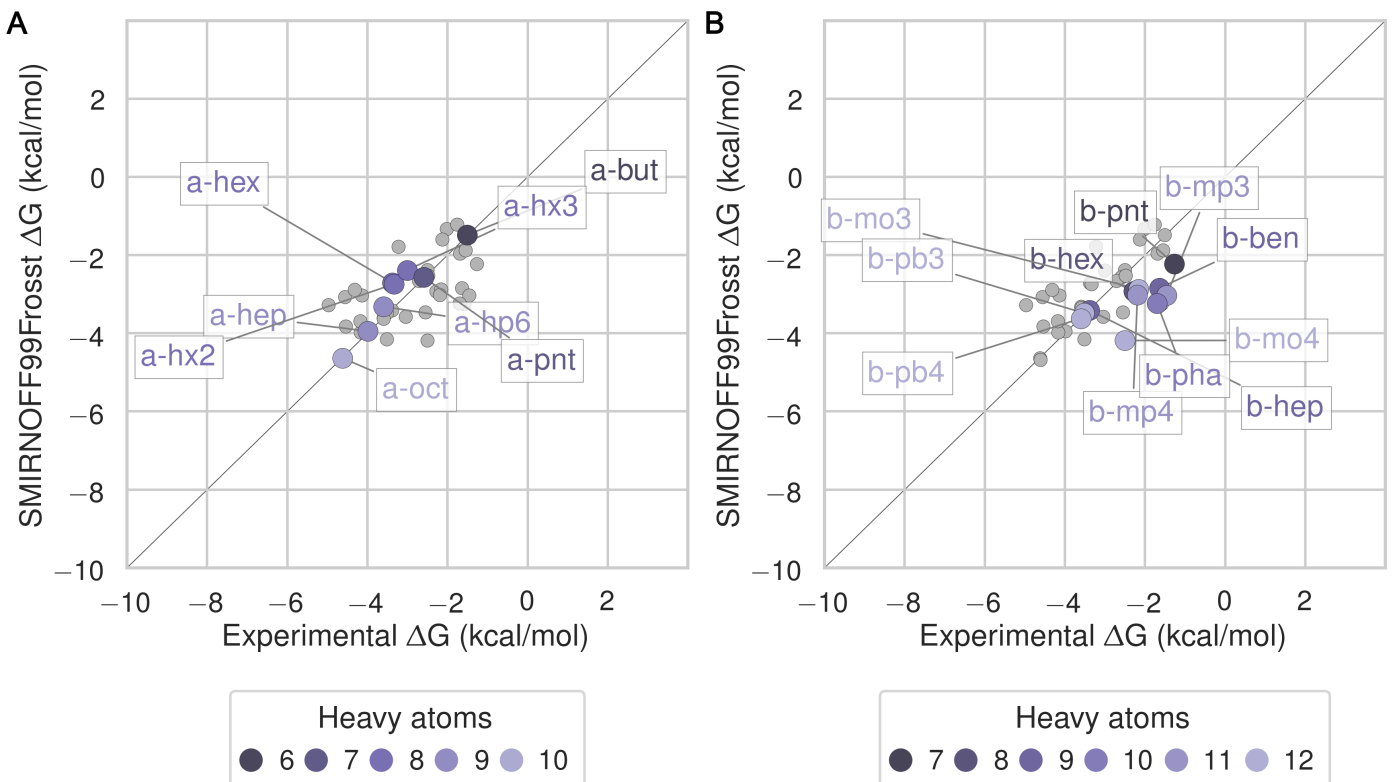


Figure 8: Binding free energy (ΔG) comparisons showing alcohols guests in color and highlighted, for α CD (A) and β CD (B). Darker colors indicates smaller molecules. Non-highlighted guests are shown as smaller gray circles.

In all cases, GAFF v1.7 tends to predict slightly weaker binding than SMIRNOFF99Frosst whereas GAFF v2.1 predicts much stronger binding for these compounds (Figures 25, 26, and 27).

Differences in force field parameters between SMIRNOFF99Frosst and GAFF

Next, we summarize the parameter differences among SMIRNOFF99Frosst, a descendant of parm99 and parm@Frosst; GAFF v1.7 (released circa March 2015 according to `gaff.dat` distributed with AMBER16); and GAFF v2.1 (which is under active development) on the parameters applied to αCD. In GAFF v2.1, the bond and angle parameters have been updated to reproduce small molecule geometries obtained from high-level quantum mechanical calculations [44]. The force constants for the bond and angle parameters were tuned to reproduce the vibrational spectra of over 600 molecules. The torsion parameters were optimized to reproduce the rotational potential energy surface of 400 model compounds. Finally, the Lennard-Jones coefficients were redeveloped to reproduce interaction energies and pure liquid properties.

Lennard-Jones

The σ and ϵ parameters are identical between SMIRNOFF99Frosst and GAFF v1.7. Note, that hydroxyl hydrogens are assigned $\sigma = 0 \text{ \AA}$ and $\epsilon = 0 \text{ kcal/mol}$ in both GAFF v1.7 and SMIRNOFF99Frosst v1.0.5, but later versions of SMIRNOFF99Frosst adopt [small \$\sigma\$ and \$\epsilon\$](#) values based on a similar atom type in parm@Frosst [45,46,47]. Compared to GAFF v2.1, SMIRNOFF99Frosst has deeper well depths for oxygens and decreased σ values for the hydroxyl hydrogens (Figure 9).

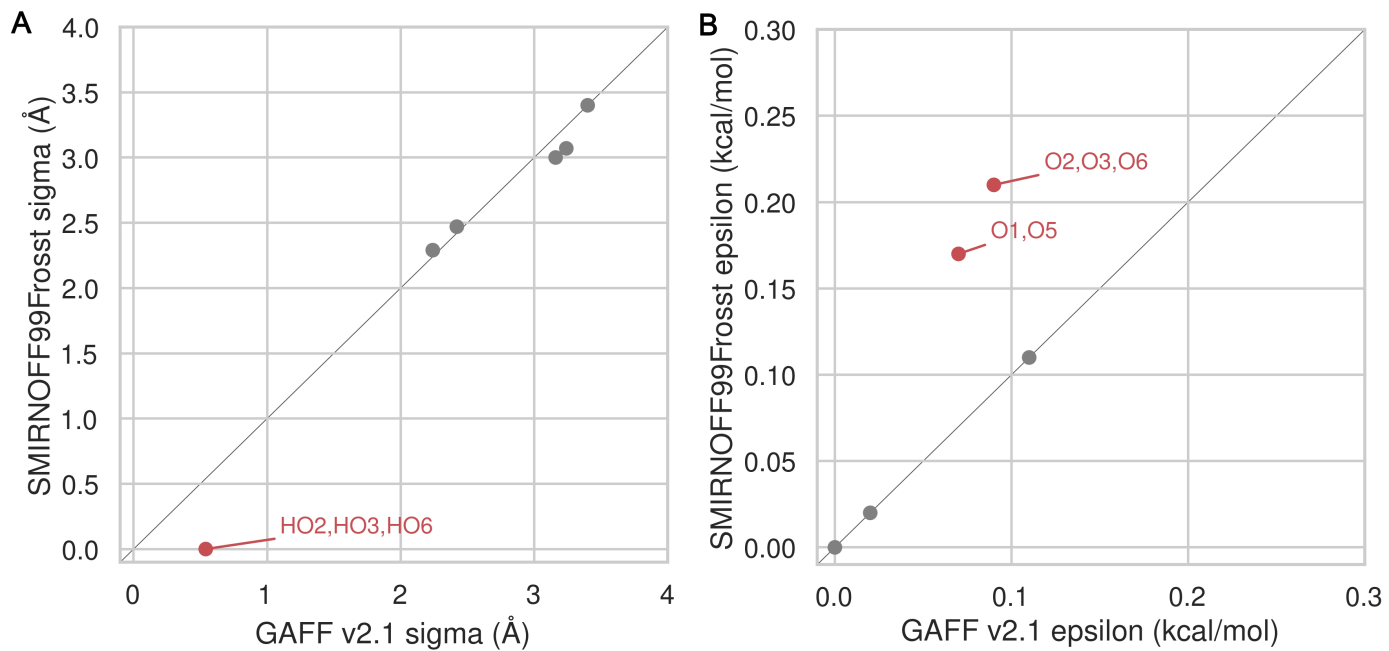


Figure 9: A comparison of Lennard-Jones nonbonded σ (A) and ϵ (B) parameters for SMIRNOFF99Frosst and GAFF v2.1. Values that differ by more than 10% are labeled in red. Atom names refer to Figure 2.

Bonded parameters

Compared to GAFF v1.7, SMIRNOFF99Frosst tends to have slightly larger bond force constants, except for the O–H hydroxyl bond force constant, which is much stronger. In GAFF v2.1, the O–H hydroxyl bond force constant is consistent with SMIRNOFF99Frosst, but the carbon-oxygen bond constants are weaker. Equilibrium bond lengths are very similar (Figure 28).

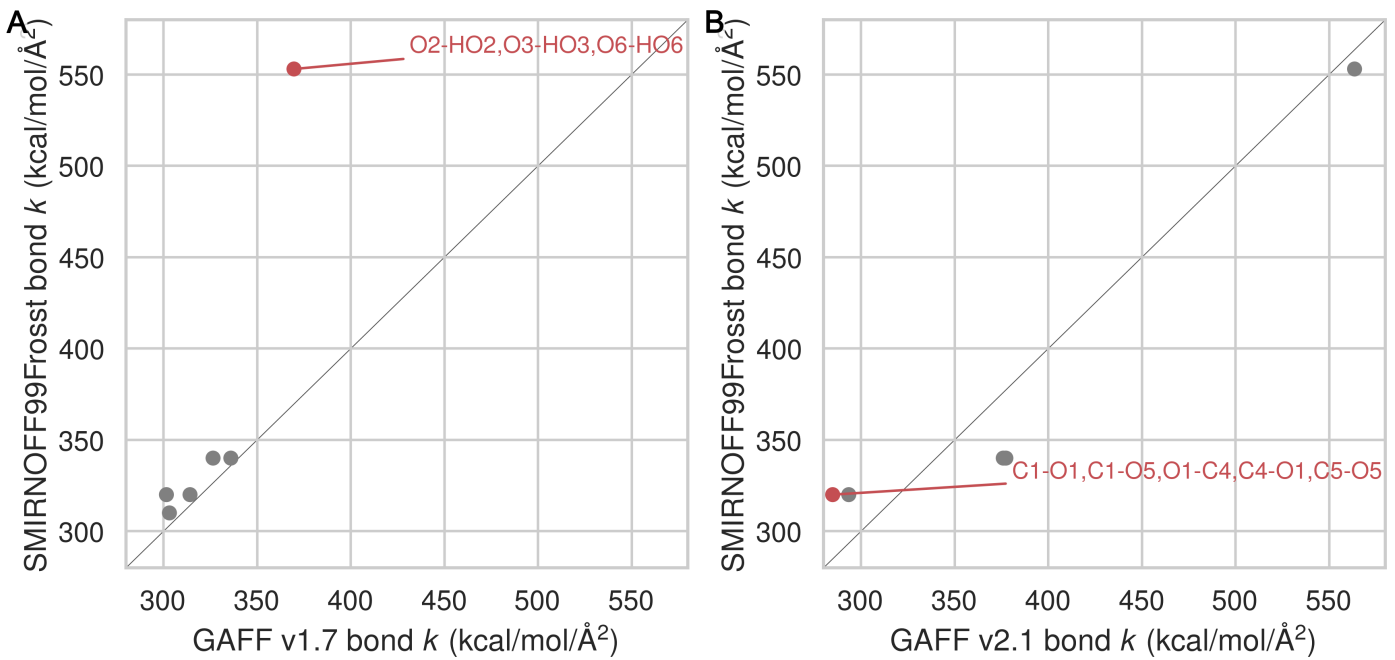


Figure 10: A comparison of bond force constants between SMIRNOFF99Frosst and GAFF v1.7 (A), or SMIRNOFF99Frosst and GAFF v2.1 (B). Values that differ by more than 10% are labeled in red. Atom names refer to Figure 2.

Angle parameters

Relative to GAFF v1.7 and GAFF v2.1, SMIRNOFF99Frosst has fewer unique angle parameters applied to αCD; several distinct parameters appear to be compressed into a single force constant, around 50 kcal/mol/rad 2 (Figure 11). These parameters correspond to C–C–C, C–O–C, and O–C–O angles. The C–C–C angles are primarily around the ring of the glucose monomer. The C–O–C angles are both around the ring and between monomers (e.g., C₁–O₁–C₄ and C₁–O₅–C₅). Weaker force constants for these parameters may lead to increased flexibility.

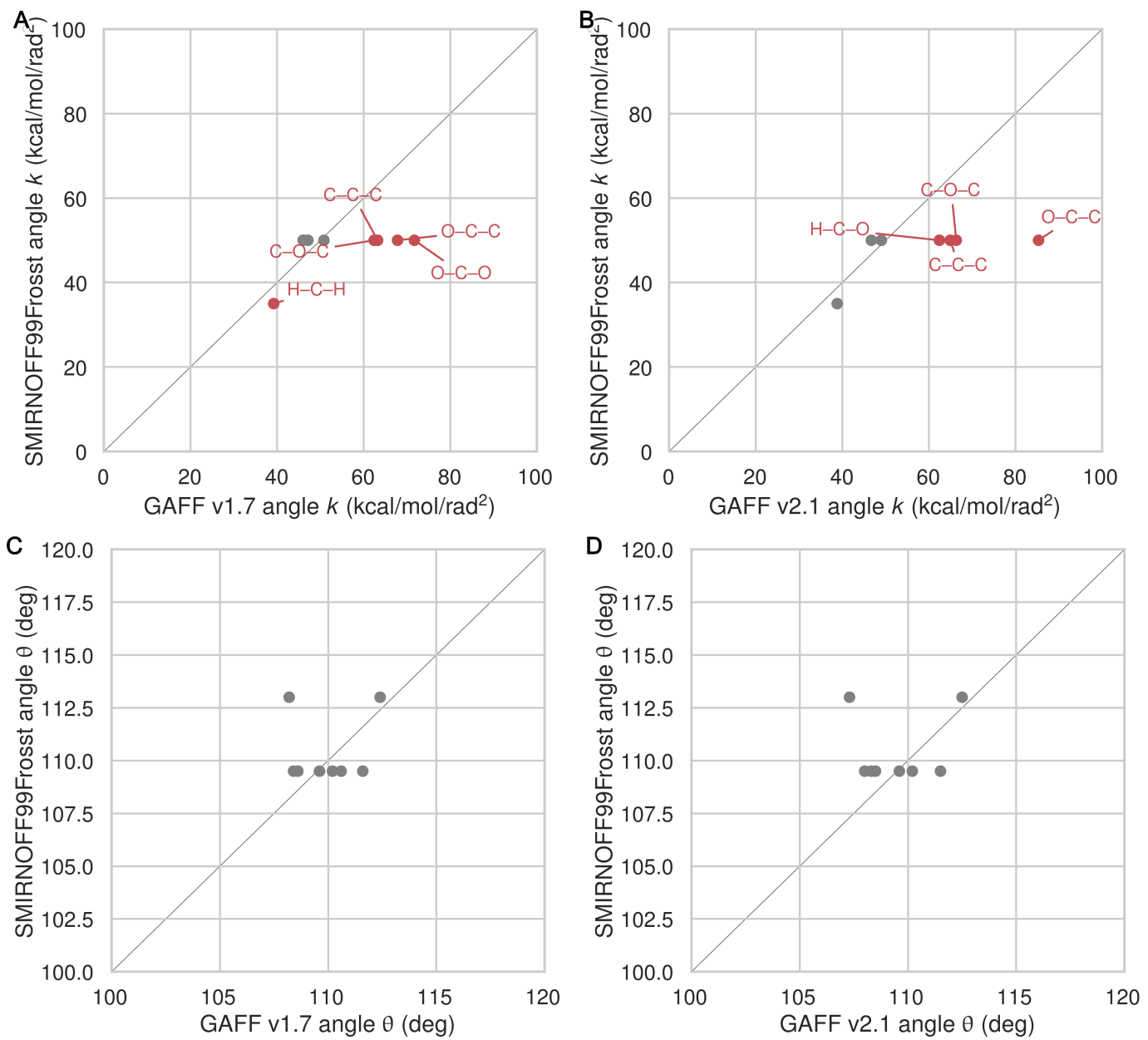


Figure 11: A comparison of angle force constants between SMIRNOFF99Frosst and GAFF v1.7 (A) or SMIRNOFF99Frosst and GAFF v2.1 (B). A comparison of equilibrium angle values SMIRNOFF99Frosst and GAFF v1.7 (C) or SMIRNOFF99Frosst and GAFF v2.1 (D). Values that differ by more than 10% are labeled in red. Precise atom names have been omitted to compress multiple angles with the same parameter values into a single label.

Dihedral parameters

The dihedral parameters in SMIRNOFF99Frosst and GAFF v1.7 are extremely similar—where differences in barrier heights occur, they are in the hundredths or thousandths of 1 kcal/mol—with the exception of the H₁–C₁–C₂–O₂ parameter (Figure 2). This dihedral corresponds to GAFF atom types h2-c3-c3-oh and SMIRKS pattern [#1:1]–[#6X4:2]–[#6X4:3]–[#8X2:4]. SMIRNOFF99Frosst applies a single term with periodicity = 1 and GAFF v1.7 applies a single term with periodicity = 3 (Table 11 and Figure 12).



Figure 12: The dihedral energy term applied to H1-C1-C2-O2 in SMIRNOFF99Frosst and GAFF v1.7. Atom names refer to Figure 2.

The dihedral parameters in GAFF v2.1 differ from those in SMIRNOFF99Frosst in a number of ways. There are several dihedrals that have a different number of terms in either force field (Table 12). This is partly due to the addition of dihedral terms with a barrier height of exactly 0.00 kcal/mol in GAFF, which are used to override wildcard parameters that might match the same atom types. For example, GAFF v2.1 applies a three term energy function to the atom types `c3-os-c3-c3`, whereas SMIRNOFF99Frosst employs a two term energy function for the SMIRKS pattern `[#6X4:1]-[#6X4:2]-[#8X2H0:3]-[#6X4:4]`, but only the terms with periodicity 2 and 3 have nonzero barrier heights in GAFF v2.1. SMIRNOFF99Frosst uses two nonzero terms to model the potential barrier for the SMIRKS pattern `[#6X4:1]-[#6X4:2]-[#8X2H1:3]-[#1:4]` yet GAFF v2.1 applies a single term with a barrier height of exactly 0.00 kcal/mol for the atom types `c3-c3-oh-ho`.

In other cases, SMIRNOFF99Frosst and GAFF v2.1 have disagreements on the barrier height after matching the periodicity and phase for a given dihedrals. It is notable that the barrier heights in GAFF v2.1 are similar in magnitude to those in SMIRNOFF99Frosst, yet GAFF v2.1 produces much more rigid structures (Table 3, Figure 14). Moreover, the dihedral differences between neighboring glucose monomers are larger in SMIRNOFF99Frosst compared to GAFF v2.1 (Table 4).

Table 3: Dihedral barrier height differences between SMIRNOFF99Frosst and GAFF v2.1 for cases where the phase and periodicity of the energy term match but the barrier height does not. Atom names refer to Figure 2.

						SMIRNOFF99Frosst	GAFF v2.1
Atom 1	Atom 2	Atom 3	Atom 4	Per	Phase	Height (kcal/mol)	Height (kcal/mol)
C1	C2	C3	C4	1	0	0.20	0.11
C1	C2	C3	C4	2	0	0.25	0.29
C1	C2	C3	C4	3	0	0.18	0.13
C1	C2	C3	O3	3	0	0.16	0.21
C1	O5	C5	H5	3	0	0.38	0.34
C2	C3	C4	C5	1	0	0.20	0.11
C2	C3	C4	C5	2	0	0.25	0.29
C2	C3	C4	C5	3	0	0.18	0.13
C3	C4	C5	C6	1	0	0.20	0.11
C3	C4	C5	C6	2	0	0.25	0.29

						SMIRNOFF99Frosst	GAFF v2.1
C3	C4	C5	C6	3	0	0.18	0.13
C4	C5	C6	O6	3	0	0.16	0.21
H1	C1	C2	H2	3	0	0.15	0.16
H2	C2	C3	H3	3	0	0.15	0.16
H2	C2	O2	HO2	3	0	0.17	0.11
H3	C3	C4	H4	3	0	0.15	0.16
H3	C3	O3	HO3	3	0	0.17	0.11
H4	C4	C5	H5	3	0	0.15	0.16
H5	C5	C6	H61	3	0	0.15	0.16
H5	C5	C6	H62	3	0	0.15	0.16
O1	C1	O5	C5	1	0	1.35	0.97
O1	C1	O5	C5	2	0	0.85	1.24
O1	C1	O5	C5	3	0	0.10	0.00
O2	C2	C3	C4	3	0	0.16	0.21
O2	C2	C3	O3	2	0	1.18	1.13
O2	C2	C3	O3	3	0	0.14	0.90
O3	C3	C4	C5	3	0	0.16	0.21
H61	C6	O6	HO6	3	0	0.17	0.11
H62	C6	O6	HO6	3	0	0.17	0.11

Table 4: Inter-residue dihedral parameter differences between SMIRNOFF99Frosst and GAFF v2.1. Atom names refer to Figure 2.

										SMIRNOFF99Frosst	GAFF v2.1	
ID	Atom 1	Res 1	Atom 2	Res 2	Atom 3	Res 3	Atom 4	Res 4	Per	Phase	Height (kcal/mol)	Height (kcal/mol)
1	C1	<i>n</i>	O1	<i>n</i>	C4	<i>n+1</i>	C3	<i>n+1</i>	1	0	–	0.00
	C1	<i>n</i>	O1	<i>n</i>	C4	<i>n+1</i>	C3	<i>n+1</i>	2	0	0.10	0.16
	C1	<i>n</i>	O1	<i>n</i>	C4	<i>n+1</i>	C3	<i>n+1</i>	3	0	0.38	0.24
2	C1	<i>n</i>	O1	<i>n</i>	C4	<i>n+1</i>	C5	<i>n+1</i>	1	0	–	0.00
	C1	<i>n</i>	O1	<i>n</i>	C4	<i>n+1</i>	C5	<i>n+1</i>	2	0	0.10	0.16
	C1	<i>n</i>	O1	<i>n</i>	C4	<i>n+1</i>	C5	<i>n+1</i>	3	0	0.38	0.24
3	C2	<i>n</i>	C1	<i>n+1</i>	O1	<i>n+1</i>	C4	<i>n+1</i>	1	0	–	0.00
	C2	<i>n</i>	C1	<i>n+1</i>	O1	<i>n+1</i>	C4	<i>n+1</i>	2	0	0.10	0.16
	C2	<i>n</i>	C1	<i>n+1</i>	O1	<i>n+1</i>	C4	<i>n+1</i>	3	0	0.38	0.24
4	O1	<i>n</i>	C4	<i>n+1</i>	C3	<i>n+1</i>	O3	<i>n+1</i>	1	0	–	0.02
	O1	<i>n</i>	C4	<i>n+1</i>	C3	<i>n+1</i>	O3	<i>n+1</i>	2	0	1.18	0.00
	O1	<i>n</i>	C4	<i>n+1</i>	C3	<i>n+1</i>	O3	<i>n+1</i>	3	0	0.14	1.01
5	O1	<i>n</i>	C4	<i>n+1</i>	C5	<i>n+1</i>	O5	<i>n+1</i>	1	0	–	0.17
	O1	<i>n</i>	C4	<i>n+1</i>	C5	<i>n+1</i>	O5	<i>n+1</i>	2	0	1.18	0.00

										SMIRNOFF99Frosst	GAFF v2.1	
	O1	n	C4	$n+1$	C5	$n+1$	O5	$n+1$	3	0	0.14	0.00

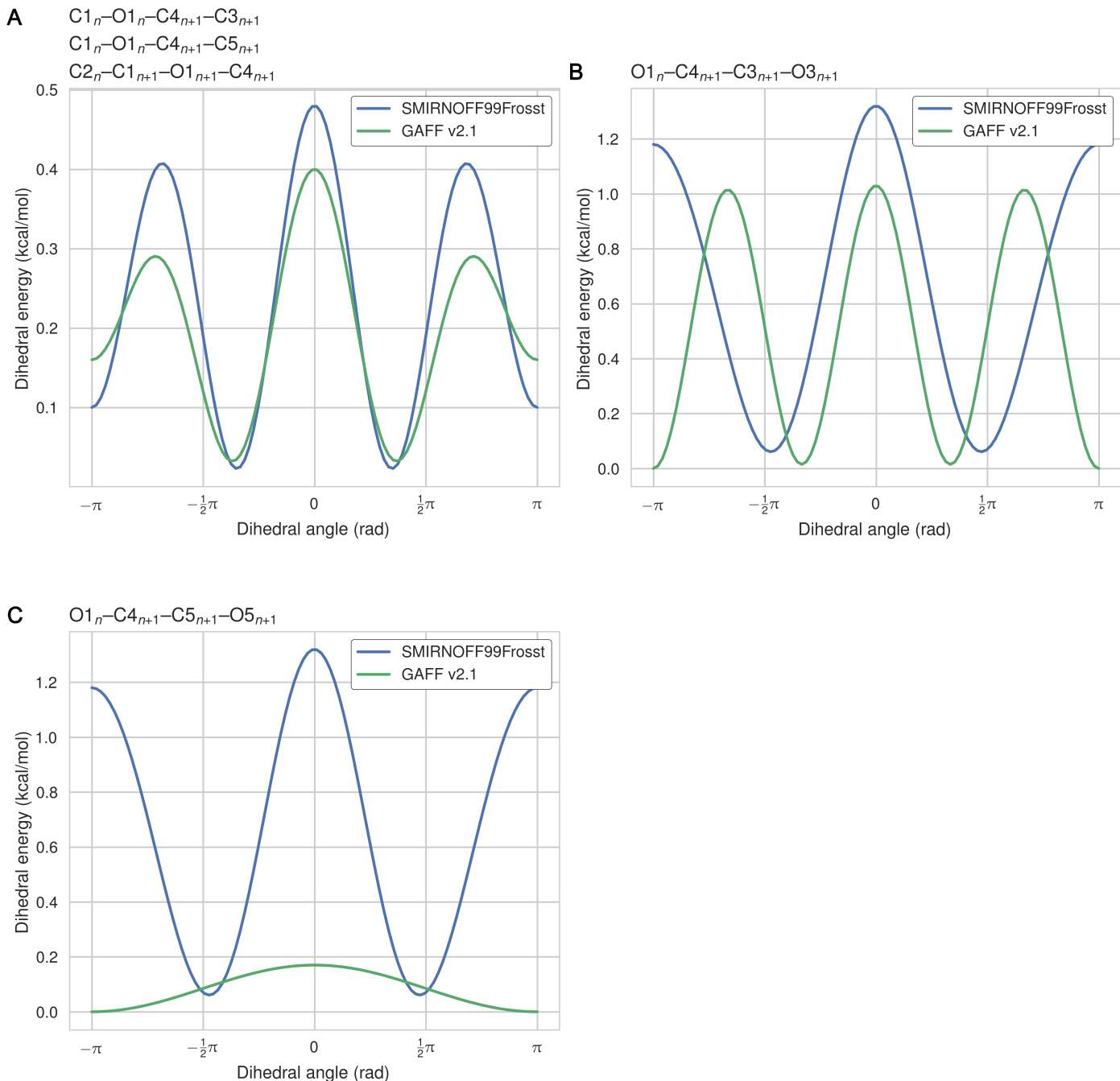


Figure 13: The dihedral energy term applied to three inter-residue dihedrals in SMIRNOFF99Frosst and GAFF v2.1. The dihedral acting on atoms $O1_n-C4_{n+1}-C5_{n+1}-O5_{n+1}$ is quite significantly different, with multiple minima and barrier heights. This dihedral partially controls the rotation of glucose monomers towards or away from the interior of the cyclodextrin cavity. Surprisingly, glucose monomers in GAFF v2.1 penetrate the open cavity much less frequently than in SMIRNOFF99Frosst, despite the lower and broader dihedral energy in GAFF v2.1. Atom names refer to Figure 2.

Structural consequences of the force field parameter differences

In both SMIRNOFF99Frosst and GAFF v1.7, the average RMSD of β CD is between 2 and 2.5 Å over 43 μ s of unrestrained simulation, in the absence of guest molecules. GAFF v2.1 is significantly more rigid, with an average RMSD less than 1.0 Å from the initial structure (Figure 14). RMSD is measured relative to a minimized structure of solvated β CD, for each force field.

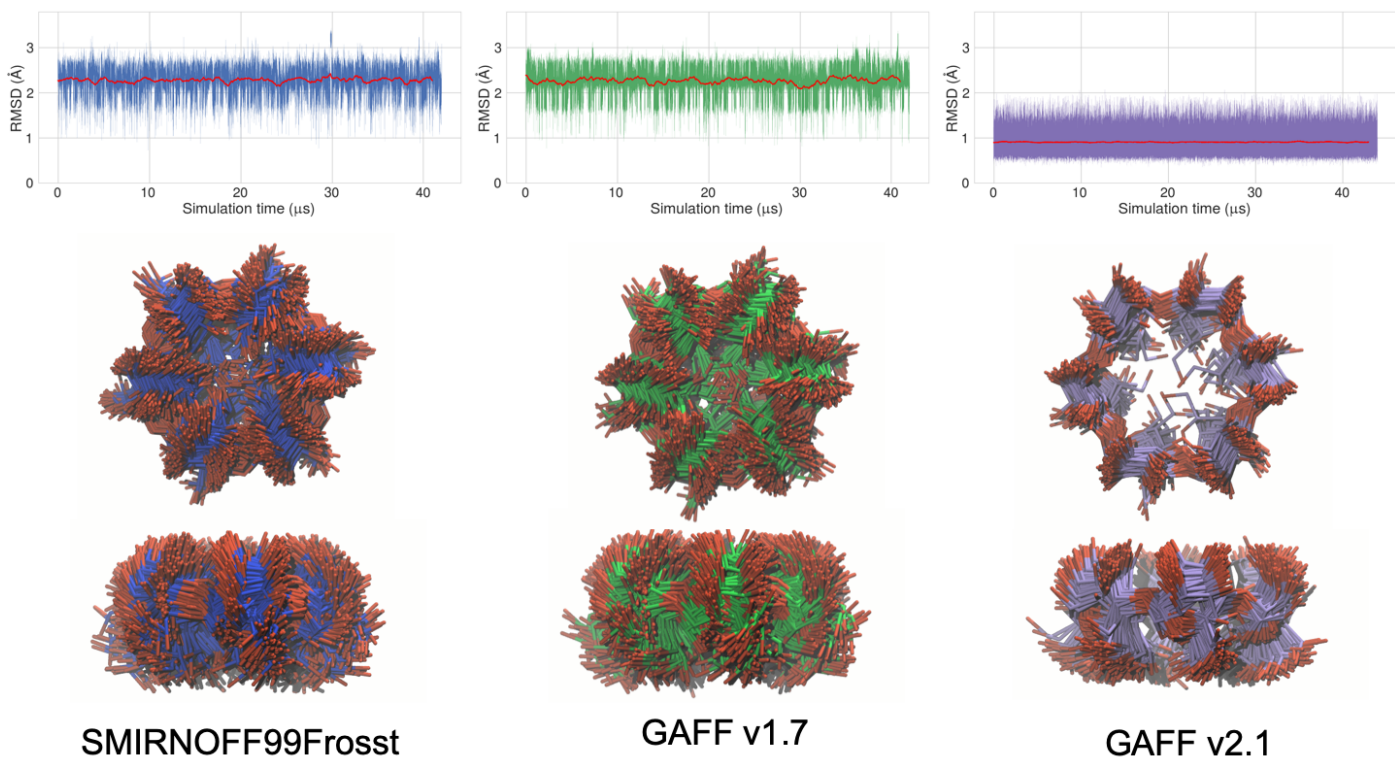


Figure 14: Top: Root mean square deviation (RMSD) of free β CD in the three force fields, all relative to the same initial structure. A 1000 frame moving average is plotted in red. Middle: to-view of the open cavity of β CD with no guest (200 snapshots over 1 μ s). Bottom: side-view of the open cavity. The carbons are colored blue in SMIRNOFF99Frosst, green in GAFF v1.7, and purple in GAFF v2.1. Hydrogen atoms have been hidden for clarity.

The “flip” pseudodihedral $O_{2n}-C_{1n}-C_{4n+1}-O_{3n+1}$ characterizes the orientation of glucose monomers relative to their neighbors. This dihedral is tightly distributed in GAFF v2.1, with all seven dihedrals having a Gaussian-like distribution, centered around -10 degrees ([15,a](#)). In contrast, simulations with both SMIRNOFF99Frosst and GAFF v1.7 report a multipeaked distribution for the dihedral, with a small amount of spread among the individual angles. At any given time point, SMIRNOFF99Frosst adopts a variety of individual pseudodihedral conformations, leading to many conformations with at least one glucose monomer inside the cyclodextrin cavity and distortion of the overall shape of the host binding pocket ([Figure 15,b-c](#)). Each pseudodihedral in GAFF v2.1 has a tight distribution; neighboring pseudodihedrals are negatively correlated with each other and positively correlated with the dihedrals on the opposite side of the ring ([Figure 15,d](#)).

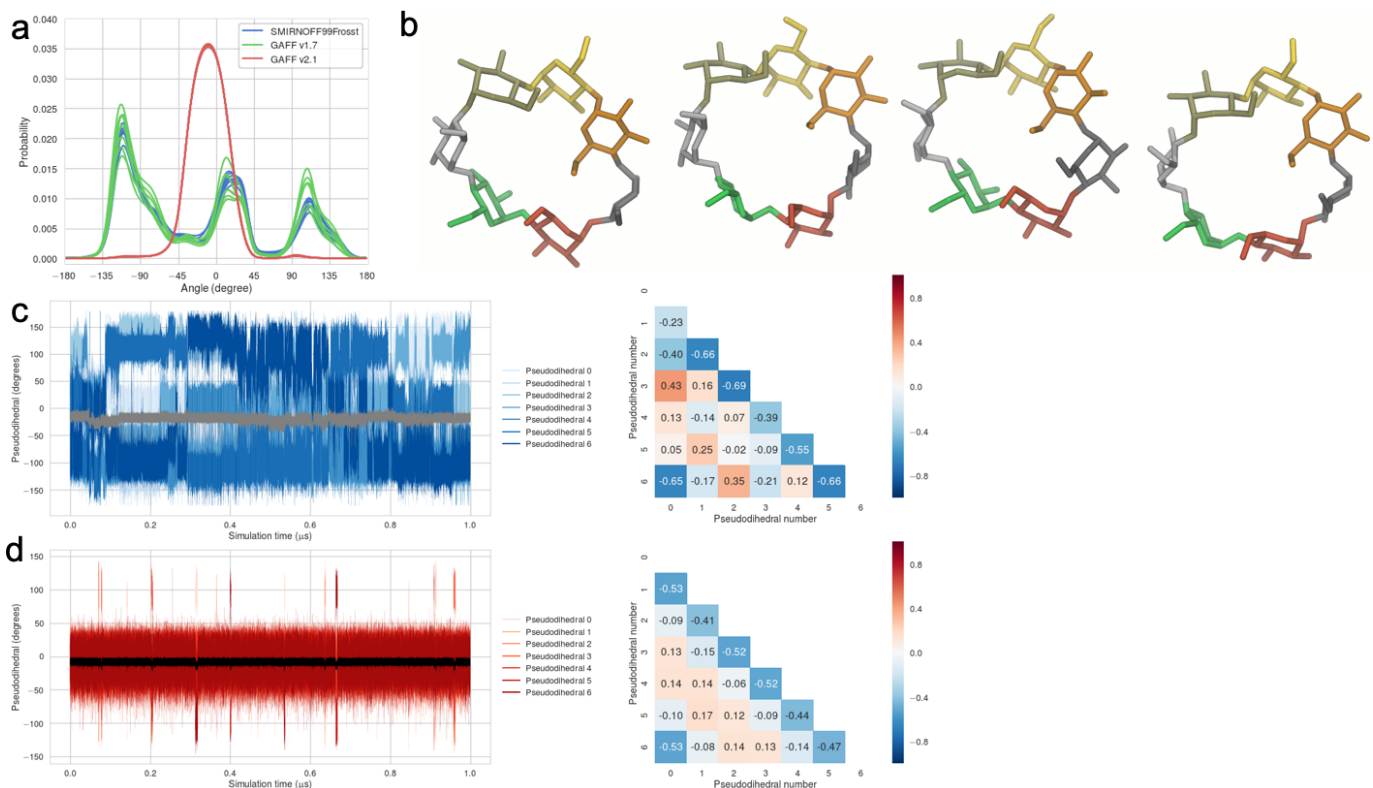


Figure 15: (a) Population histograms of the pseudodihedral in free β CD, averaged over 43 μ s, for each force field; one curve is drawn for each pseudodihedral in β CD. (b) Renderings of β CD in GAFF v1.7 which have the similar mean pseudodihedral values but very different individual pseudodihedral values. (c) Left: The timeseries of pseudodihedral values in SMIRNOFF99Frosst during the $b\text{-}chp\text{-}p$ simulation. The average value is drawn in grey. Right: The correlation between pseudodihedrals in the β CD ring with SMIRNOFF99Frosst. (d) The same as panel (c) except using GAFF v2.1.

Discussion

As a terse representation of a GAFF-like force field, SMIRNOFF99Frosst performs remarkably well. Despite having far fewer parameters than GAFF v1.7 and GAFF v2.1, SMIRNOFF99Frosst performs as well as GAFF v1.7 and better than GAFF v2.1 on estimated binding free energies of small molecules to α CD and β CD, based on the mean signed error relative to experiment. Moreover, SMIRNOFF99Frosst performs better than either GAFF v1.7 or GAFF v2.1 on predicted binding enthalpies, with a mean signed error less than 1 kcal/mol. GAFF v2.1 has excellent agreement with experiment on predicted binding entropy, followed by SMIRNOFF99Frosst and then GAFF v1.7. Taken together, these results support the notion that a simpler force field, based on direct chemical perception and fewer “exceptions to the rules,” are as accurate as force fields that have been hand-tuned over decades of use. The reduction in the number of parameters, and the simplification of the force field specification, will make it easier to iteratively refine and optimize SMIRNOFF99Frosst against experimental data and the results of quantum mechanical calculations.

It is notable that both SMIRNOFF99Frosst and GAFF v1.7 result in excessively flexible cyclodextrin hosts. It has been shown that there are 2–7 H_2O inside α CD and 8–11 H_2O molecules inside β CD [18, 48]. It is likely that simulations with SMIRNOFF99Frosst and GAFF v1.7 result in fewer resident waters inside the cyclodextrin cavity due to intrusions from glucose units. Furthermore, it is known that sugars and conjugated carbohydrates are especially difficult for many “general” force fields, due to the highly polar bonds in sugars, the number of chiral centers, and the large structural differences between chiral isomers [49].

The combination of X-ray and NMR data suggest that the specialized q4md-CD [50] force field, and the rigid GAFF v2.1 [31] force field, better model the flexibility of the CD cavity. Cézard, et al. present strong NMR evidence that the vicinal 3J H5–H6' (atom names H5–H62 in Figure 2) and 3J H5–H6''(atom names H5–H61) coupling show minimal fluctuation in distance over a number of timescales, suggesting little

change in the population of rotamers [50]. This is also evident in X-ray structures, where the rigidity of the cyclodextrin ring is retained as long as water is present in the cavity and the torsional angles between adjacent glycouril units show surprisingly small variance [48]. The CHARMM36 force field displays similar structural dynamics to q4md-CD, with certain GROMOS force fields even more rigid than those [51]. The lack of rigidity is associated with an underestimation of the binding enthalpy and an overestimation of the binding entropy; SMIRNOFF99Frosst has a ΔH MSE = 0.77 kcal/mol and $-\Delta S$ MSE = -0.78 kcal/mol whereas the more rigid GAFF v2.1 results in ΔH MSE = -1.64 kcal/mol and $-\Delta S$ MSE = 0.08 kcal/mol. It is especially notable that GAFF v2.1 has the best overall correlations.

As SMIRNOFF99Frosst grows beyond a small molecule force field, it will be important to include sugars and other carbohydrates in the training sets used to develop parameters. This will be especially useful for modeling physiologically relevant protein structures, such as proteoglycans and glycopeptides.

The results presented in this manuscript demonstrate that host-guest binding thermodynamics can be used to benchmark force fields, diagnose issues with parameters applied to specific functional groups, and suggest directions for improvements.

Discussion is still rough around the edges. Two immediate thoughts: I could focus more about how SMIRNOFF99Frosst does modeling cyclodextrins (currently the middle paragraph of this section). Or, I could be more circumspect, connecting with the Introduction, and mentioning that host-guest systems are good models and identify force field errors. This section would benefit from some concrete input.

Code and data availability

- [GitHub repository](#) used to convert AMBER input files from GAFF force field to SMIRNOFF99Frosst.
- [GitHub repository](#) for setting up the attach-pull-release calculations using `paprika` version 0.0.3.
- [GitHub repository](#) for analyzing the simulations and generating the plots in this manuscript.
- [GitHub repository](#) for the Open Force Field group containing the toolkit and force field XML file.

Author contributions

Conceptualization, DRS, NMH, JDC, MKG; Methodology, DRS, NMH; Software, DRS, NMH; Formal Analysis, DRS, NMH, JDC, MKG; Investigation, DRS, NMH; Resources, MKG, JDC; Data Curation, DRS, NMH; Writing-Original Draft, DRS, NMH; Writing - Review and Editing, DRS, NMH, JDC, MKG, LPW; Visualization, DRS; Supervision, JDC, MKG; Project Administration, MKG; Funding Acquisition, MKG.

Acknowledgments

Disclosures

The authors declare the following competing financial interest(s): MKG has an equity interest in and is a cofounder and scientific advisor of VeraChem LLC.

List of abbreviations

APR, attach-pull-release; CD, cyclodextrin; GAFF, Generalized AMBER Force Field

References

1. Overview of the SAMPL6 host–guest binding affinity prediction challenge

Andrea Rizzi, Steven Murkli, John N. McNeill, Wei Yao, Matthew Sullivan, Michael K. Gilson, Michael W. Chiu, Lyle Isaacs, Bruce C. Gibb, David L. Mobley, John D. Chodera

Journal of Computer-Aided Molecular Design (2018-10) <https://doi.org/gfpzh5>

DOI: [10.1007/s10822-018-0170-6](https://doi.org/10.1007/s10822-018-0170-6) · PMID: [30415285](https://pubmed.ncbi.nlm.nih.gov/30415285/) · PMCID: [PMC6301044](https://pubmed.ncbi.nlm.nih.gov/PMC6301044/)

2. Attach-Pull-Release Calculations of Ligand Binding and Conformational Changes on the First BRD4 Bromodomain

Germano Heinzelmann, Niel M. Henriksen, Michael K. Gilson

Journal of Chemical Theory and Computation (2017-05-31) <https://doi.org/gbpj4m>

DOI: [10.1021/acs.jctc.7b00275](https://doi.org/10.1021/acs.jctc.7b00275) · PMID: [28564537](https://pubmed.ncbi.nlm.nih.gov/28564537/) · PMCID: [PMC5541932](https://pubmed.ncbi.nlm.nih.gov/PMC5541932/)

3. Computation of protein–ligand binding free energies using quantum mechanical bespoke force fields

Daniel J. Cole, Israel Cabeza de Vaca, William L. Jorgensen

MedChemComm (2019) <https://doi.org/gfz353>

DOI: [10.1039/c9md00017h](https://doi.org/10.1039/c9md00017h)

4. Predictions of Ligand Selectivity from Absolute Binding Free Energy Calculations

Matteo Aldeghi, Alexander Heifetz, Michael J. Bodkin, Stefan Knapp, Philip C. Biggin

Journal of the American Chemical Society (2017-01-09) <https://doi.org/f9kr6h>

DOI: [10.1021/jacs.6b11467](https://doi.org/10.1021/jacs.6b11467) · PMID: [28009512](https://pubmed.ncbi.nlm.nih.gov/28009512/) · PMCID: [PMC5253712](https://pubmed.ncbi.nlm.nih.gov/PMC5253712/)

5. Accurate and Reliable Prediction of Relative Ligand Binding Potency in Prospective Drug Discovery by Way of a Modern Free-Energy Calculation Protocol and Force Field

Lingle Wang, Yujie Wu, Yuqing Deng, Byungchan Kim, Levi Pierce, Goran Krilov, Dmitry Lupyan, Shaughnessy Robinson, Markus K. Dahlgren, Jeremy Greenwood, ... Robert Abel

Journal of the American Chemical Society (2015-02-12) <https://doi.org/f64pdz>

DOI: [10.1021/ja512751q](https://doi.org/10.1021/ja512751q) · PMID: [25625324](https://pubmed.ncbi.nlm.nih.gov/25625324/)

6. OPLS3e: Extending Force Field Coverage for Drug-Like Small Molecules

Katarina Roos, Chuanjie Wu, Wolfgang Damm, Mark Reboul, James M. Stevenson, Chao Lu, Markus K. Dahlgren, Sayan Mondal, Wei Chen, Lingle Wang, ... Edward D. Harder

Journal of Chemical Theory and Computation (2019-02-15) <https://doi.org/gfvpnf>

DOI: [10.1021/acs.jctc.8b01026](https://doi.org/10.1021/acs.jctc.8b01026) · PMID: [30768902](https://pubmed.ncbi.nlm.nih.gov/30768902/)

7. Validation of AMBER/GAFF for Relative Free Energy Calculations

Lin Song, Tai-Sung Lee, Chun Zhu, Darrin M. York, Kenneth M. Merz Jr.

American Chemical Society (ACS) (2019-02-04) <https://doi.org/gf22kq>

DOI: [10.26434/chemrxiv.7653434](https://doi.org/10.26434/chemrxiv.7653434)

8. Overview of the SAMPL5 host–guest challenge: Are we doing better?

Jian Yin, Niel M. Henriksen, David R. Slochower, Michael R. Shirts, Michael W. Chiu, David L. Mobley, Michael K. Gilson

Journal of Computer-Aided Molecular Design (2016-09-22) <https://doi.org/f9m82x>

DOI: [10.1007/s10822-016-9974-4](https://doi.org/10.1007/s10822-016-9974-4) · PMID: [27658802](https://pubmed.ncbi.nlm.nih.gov/27658802/) · PMCID: [PMC5241188](https://pubmed.ncbi.nlm.nih.gov/PMC5241188/)

9. The Movable Type Method Applied to Protein–Ligand Binding

Zheng Zheng, Melek N. Ucisik, Kenneth M. Merz

10. Blinded predictions of standard binding free energies: lessons learned from the SAMPL6 challenge

Michail Papadourakis, Stefano Bosisio, Julien Michel

Journal of Computer-Aided Molecular Design (2018-08-29) <https://doi.org/gfpbrc>

DOI: [10.1007/s10822-018-0154-6](https://doi.org/10.1007/s10822-018-0154-6) · PMID: [30159717](#)

11. Resolving the problem of trapped water in binding cavities: prediction of host–guest binding free energies in the SAMPL5 challenge by funnel metadynamics

Soumendranath Bhakat, Pär Söderhjelm

Journal of Computer-Aided Molecular Design (2016-08-29) <https://doi.org/f9m894>

DOI: [10.1007/s10822-016-9948-6](https://doi.org/10.1007/s10822-016-9948-6) · PMID: [27573983](#) · PMCID: [PMC5239820](#)

12. Absolute binding free energies for octa-acids and guests in SAMPL5

Florentina Tofoleanu, Juyong Lee, Frank C. Pickard IV, Gerhard König, Jing Huang, Minkyung Baek, Chaok Seok, Bernard R. Brooks

Journal of Computer-Aided Molecular Design (2016-09-30) <https://doi.org/f9m9c2>

DOI: [10.1007/s10822-016-9965-5](https://doi.org/10.1007/s10822-016-9965-5) · PMID: [27696242](#) · PMCID: [PMC6472255](#)

13. Computational Calorimetry: High-Precision Calculation of Host–Guest Binding Thermodynamics

Niel M. Henriksen, Andrew T. Fenley, Michael K. Gilson

Journal of Chemical Theory and Computation (2015-08-26) <https://doi.org/f7q3mj>

DOI: [10.1021/acs.jctc.5b00405](https://doi.org/10.1021/acs.jctc.5b00405) · PMID: [26523125](#) · PMCID: [PMC4614838](#)

14. Prediction of CB[8] host–guest binding free energies in SAMPL6 using the double-decoupling method

Kyungreem Han, Phillip S. Hudson, Michael R. Jones, Naohiro Nishikawa, Florentina Tofoleanu, Bernard R. Brooks

Journal of Computer-Aided Molecular Design (2018-08-06) <https://doi.org/gfpzp2>

DOI: [10.1007/s10822-018-0144-8](https://doi.org/10.1007/s10822-018-0144-8) · PMID: [30084077](#) · PMCID: [PMC6347468](#)

15. Comparison of the umbrella sampling and the double decoupling method in binding free energy predictions for SAMPL6 octa-acid host–guest challenges

Naohiro Nishikawa, Kyungreem Han, Xiongwu Wu, Florentina Tofoleanu, Bernard R. Brooks

Journal of Computer-Aided Molecular Design (2018-10) <https://doi.org/gfz352>

DOI: [10.1007/s10822-018-0166-2](https://doi.org/10.1007/s10822-018-0166-2) · PMID: [30324304](#) · PMCID: [PMC6413509](#)

16. Detailed potential of mean force studies on host–guest systems from the SAMPL6 challenge

Lin Frank Song, Nupur Bansal, Zheng Zheng, Kenneth M. Merz

Journal of Computer-Aided Molecular Design (2018-08-24) <https://doi.org/gfpw5t>

DOI: [10.1007/s10822-018-0153-7](https://doi.org/10.1007/s10822-018-0153-7) · PMID: [30143917](#)

17. The SAMPL4 host–guest blind prediction challenge: an overview

Hari S. Muddana, Andrew T. Fenley, David L. Mobley, Michael K. Gilson

Journal of Computer-Aided Molecular Design (2014-03-06) <https://doi.org/f5585s>

DOI: [10.1007/s10822-014-9735-1](https://doi.org/10.1007/s10822-014-9735-1) · PMID: [24599514](#) · PMCID: [PMC4053502](#)

18. Structures of the Common Cyclodextrins and Their Larger Analogues Beyond the Doughnut

Wolfram Saenger, Joël Jacob, Katrin Gessler, Thomas Steiner, Daniel Hoffmann, Haruyo Sanbe, Kyoko Koizumi, Steven M. Smith, Takeshi Takaha

Chemical Reviews (1998-07) <https://doi.org/dgz7hm>
DOI: [10.1021/cr9700181](https://doi.org/10.1021/cr9700181)

19. Toward Expanded Diversity of Host–Guest Interactions via Synthesis and Characterization of Cyclodextrin Derivatives

K. Kellett, S. A. Kantonen, B. M. Duggan, M. K. Gilson
Journal of Solution Chemistry (2018-06-04) <https://doi.org/gfp949>
DOI: [10.1007/s10953-018-0769-1](https://doi.org/10.1007/s10953-018-0769-1)

20. Cyclodextrins and their uses: a review

E. M. Martin Del Valle
Process Biochemistry (2004-05) <https://doi.org/bxthjg>
DOI: [10.1016/s0032-9592\(03\)00258-9](https://doi.org/10.1016/s0032-9592(03)00258-9)

21. Escaping Atom Types in Force Fields Using Direct Chemical Perception

David L. Mobley, Caitlin C. Bannan, Andrea Rizzi, Christopher I. Bayly, John D. Chodera, Victoria T. Lim, Nathan M. Lim, Kyle A. Beauchamp, David R. Slochower, Michael R. Shirts, ... Peter K. Eastman
Journal of Chemical Theory and Computation (2018-10-11) <https://doi.org/gffnf3>
DOI: [10.1021/acs.jctc.8b00640](https://doi.org/acs.jctc.8b00640) · PMID: [30351006](https://pubmed.ncbi.nlm.nih.gov/30351006/) · PMCID: [PMC6245550](https://pubmed.ncbi.nlm.nih.gov/PMC6245550/)

22. Open Force Field Initiative

The Open Force Field Initiative
<https://openforcefield.org/>

23. A Modified Version of the Cornell et al. Force Field with Improved Sugar Pucker Phases and Helical Repeat

Thomas E. Cheatham III, Piotr Cieplak, Peter A. Kollman
Journal of Biomolecular Structure and Dynamics (1999-02) <https://doi.org/gfzp4j>
DOI: [10.1080/07391102.1999.10508297](https://doi.org/10.1080/07391102.1999.10508297) · PMID: [10217454](https://pubmed.ncbi.nlm.nih.gov/10217454/)

24. An Informal AMBER Small Molecule Force Field:

parm@Frosst http://www.ccl.net/cca/data/parm_at_Frosst/

25. AMBER 2018

D. A. Case, D. S. Cerutti, T. E. III Cheatham, T. A. Darden, R. E. Duke, H. Gohlke, A. W. Goetz, D. Greene, N. Homeyer, S. Izadi, ... V. W.D. Cruzeiro

26. Daylight>SMIRKS Tutorial https://daylight.com/dayhtml_tutorials/languages/smirks/

27. Development and testing of a general amber force field

Junmei Wang, Romain M. Wolf, James W. Caldwell, Peter A. Kollman, David A. Case
Journal of Computational Chemistry (2004) <https://doi.org/cdmcnb>
DOI: [10.1002/jcc.20035](https://doi.org/10.1002/jcc.20035) · PMID: [15116359](https://pubmed.ncbi.nlm.nih.gov/15116359/)

28. A general small molecule force field descended from AMBER99 and parm@Frosst, available in the SMIRNOFF format: openforcefield/smirkoff99Frosst

Open Force Field Initiative
(2019-05-19) <https://github.com/openforcefield/smirkoff99Frosst>

29. Open Force Field Roadmap

Michael R Shirts, John Damon Chodera, David L Mobley, Michael K Gilson, Lee-Ping Wang
Unpublished (2019) <https://doi.org/gf2stw>
DOI: [10.13140/rg.2.2.27587.86562](https://doi.org/10.13140/rg.2.2.27587.86562)

30. Thermodynamic and Nuclear Magnetic Resonance Study of the Reactions of α - and β -Cyclodextrin with Acids, Aliphatic Amines, and Cyclic Alcohols

Mikhail V. Rekharsky, Martin P. Mayhew, Robert N. Goldberg, Philip D. Ross, Yuko Yamashoji, Yoshihisa Inoue

The Journal of Physical Chemistry B (1997-01) <https://doi.org/cmwfwn>

DOI: [10.1021/jp962715n](https://doi.org/10.1021/jp962715n)

31. Evaluating Force Field Performance in Thermodynamic Calculations of Cyclodextrin Host-Guest Binding: Water Models, Partial Charges, and Host Force Field Parameters

Niel M. Henriksen, Michael K. Gilson

Journal of Chemical Theory and Computation (2017-07-11) <https://doi.org/gd2z2t>

DOI: [10.1021/acs.jctc.7b00359](https://doi.org/10.1021/acs.jctc.7b00359) · PMID: [28696692](https://pubmed.ncbi.nlm.nih.gov/28696692/) · PMCID: [PMC5606194](https://pubmed.ncbi.nlm.nih.gov/PMC5606194/)

32. Chiral Recognition Thermodynamics of β -Cyclodextrin: The Thermodynamic Origin of Enantioselectivity and the Enthalpy–Entropy Compensation Effect

Mikhail Rekharsky, Yoshihisa Inoue

Journal of the American Chemical Society (2000-05) <https://doi.org/c2tvdg>

DOI: [10.1021/ja9921118](https://doi.org/10.1021/ja9921118)

33. Fast, efficient generation of high-quality atomic charges. AM1-BCC model: II. Parameterization and validation

Araz Jakalian, David B. Jack, Christopher I. Bayly

Journal of Computational Chemistry (2002-10-18) <https://doi.org/cktk6g>

DOI: [10.1002/jcc.10128](https://doi.org/10.1002/jcc.10128) · PMID: [12395429](https://pubmed.ncbi.nlm.nih.gov/12395429/)

34. Fast, efficient generation of high-quality atomic charges. AM1-BCC model: I. Method

Araz Jakalian, Bruce L. Bush, David B. Jack, Christopher I. Bayly

Journal of Computational Chemistry (2000-01-30) <https://doi.org/cvvpkv>

DOI: [10.1002/\(sici\)1096-987x\(20000130\)21:2<132::aid-jcc5>3.0.co;2-p](https://doi.org/10.1002/(sici)1096-987x(20000130)21:2<132::aid-jcc5>3.0.co;2-p)

35. Comparison of simple potential functions for simulating liquid water

William L. Jorgensen, Jayaraman Chandrasekhar, Jeffry D. Madura, Roger W. Impey, Michael L. Klein

The Journal of Chemical Physics (1983-07-15) <https://doi.org/dg9sq8>

DOI: [10.1063/1.445869](https://doi.org/10.1063/1.445869)

36. Determination of Alkali and Halide Monovalent Ion Parameters for Use in Explicitly Solvated Biomolecular Simulations

In Suk Joung, Thomas E. Cheatham III

The Journal of Physical Chemistry B (2008-07) <https://doi.org/cgwnj7>

DOI: [10.1021/jp8001614](https://doi.org/10.1021/jp8001614) · PMID: [18593145](https://pubmed.ncbi.nlm.nih.gov/18593145/) · PMCID: [PMC2652252](https://pubmed.ncbi.nlm.nih.gov/PMC2652252/)

37. Lessons learned from comparing molecular dynamics engines on the SAMPL5 dataset

Michael R. Shirts, Christoph Klein, Jason M. Swails, Jian Yin, Michael K. Gilson, David L. Mobley, David A. Case, Ellen D. Zhong

Journal of Computer-Aided Molecular Design (2016-10-27) <https://doi.org/f9m3wn>

DOI: [10.1007/s10822-016-9977-1](https://doi.org/10.1007/s10822-016-9977-1) · PMID: [27787702](https://pubmed.ncbi.nlm.nih.gov/27787702/) · PMCID: [PMC5581938](https://pubmed.ncbi.nlm.nih.gov/PMC5581938/)

38. Overcoming dissipation in the calculation of standard binding free energies by ligand extraction

Camilo Velez-Vega, Michael K. Gilson

Journal of Computational Chemistry (2013-08) <https://doi.org/gbdv9w>

DOI: [10.1002/jcc.23398](https://doi.org/10.1002/jcc.23398) · PMID: [24038118](https://pubmed.ncbi.nlm.nih.gov/24038118/) · PMCID: [PMC3932244](https://pubmed.ncbi.nlm.nih.gov/PMC3932244/)

39. Bridging Calorimetry and Simulation through Precise Calculations of Cucurbituril–Guest Binding Enthalpies

Andrew T. Fenley, Niel M. Henriksen, Hari S. Muddana, Michael K. Gilson

Journal of Chemical Theory and Computation (2014-08) <https://doi.org/f6hv4x>

DOI: [10.1021/ct5004109](https://doi.org/10.1021/ct5004109) · PMID: [25221445](https://pubmed.ncbi.nlm.nih.gov/25221445/) · PMCID: [PMC4159218](https://pubmed.ncbi.nlm.nih.gov/PMC4159218/)

40. The Amber Molecular Dynamics Package(2019) <http://www.ambermd.org>

41. Long-Time-Step Molecular Dynamics through Hydrogen Mass Repartitioning

Chad W. Hopkins, Scott Le Grand, Ross C. Walker, Adrian E. Roitberg

Journal of Chemical Theory and Computation (2015-03-30) <https://doi.org/f697mk>

DOI: [10.1021/ct5010406](https://doi.org/10.1021/ct5010406) · PMID: [26574392](https://pubmed.ncbi.nlm.nih.gov/26574392/)

42. Nonlinear scaling schemes for Lennard-Jones interactions in free energy calculations

Thomas Steinbrecher, David L. Mobley, David A. Case

The Journal of Chemical Physics (2007-12-07) <https://doi.org/fc7n55>

DOI: [10.1063/1.2799191](https://doi.org/10.1063/1.2799191) · PMID: [18067350](https://pubmed.ncbi.nlm.nih.gov/18067350/)

43. Error estimates on averages of correlated data

H. Flyvbjerg, H. G. Petersen

The Journal of Chemical Physics (1989-07) <https://doi.org/bjpm5j>

DOI: [10.1063/1.457480](https://doi.org/10.1063/1.457480)

44. A stripped-down set of just antechamber, sqm, and tleap.: choderalab/ambermini

Chodera lab // Memorial Sloan Kettering Cancer Center

(2017-11-15) <https://github.com/choderalab/ambermini>

45. Add hydroxyl hydrogen radii, remove generics, update for 1.0.7 release by davidlmobley · Pull Request #74 · openforcefield/smirnoff99Frosst

GitHub

<https://github.com/openforcefield/smirnoff99Frosst/pull/74>

46. Remove generics, add hydrogen radii, rename fxml files by davidlmobley · Pull Request #101 · openforcefield/openforcefield

GitHub

<https://github.com/openforcefield/openforcefield/pull/101>

47. Adjust hydroxyl hydrogen to have a small radius, requires more research · Issue #61 · openforcefield/smirnoff99Frosst

GitHub

<https://github.com/openforcefield/smirnoff99Frosst/issues/61>

48. Topography of cyclodextrin inclusion complexes. 8. Crystal and molecular structure of the .alpha.-cyclodextrin-methanol-pentahydrate complex. Disorder in a hydrophobic cage

B. Hingerty, W. Saenger

Journal of the American Chemical Society (1976-05) <https://doi.org/cmfv5v>

DOI: [10.1021/ja00427a050](https://doi.org/10.1021/ja00427a050)

49. Carbohydrate force fields

B. Lachele Foley, Matthew B. Tessier, Robert J. Woods

Wiley Interdisciplinary Reviews: Computational Molecular Science (2011-10-31) <https://doi.org/fcxc66>

DOI: [10.1002/wcms.89](https://doi.org/10.1002/wcms.89) · PMID: [25530813](https://pubmed.ncbi.nlm.nih.gov/25530813/) · PMCID: [PMC4270206](https://pubmed.ncbi.nlm.nih.gov/PMC4270206/)

50. Molecular dynamics studies of native and substituted cyclodextrins in different media: 1. Charge derivation and force field performances

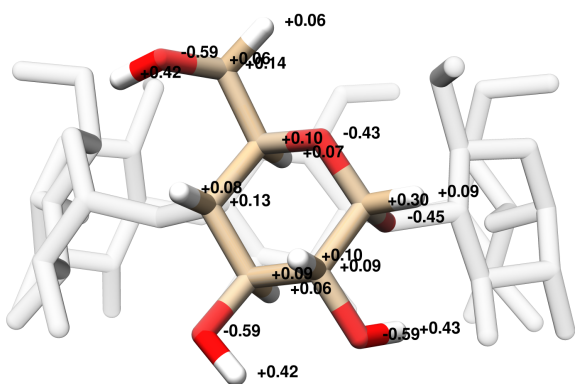
Christine Cézard, Xavier Trivelli, Frédéric Aubry, Florence Djedai ni-Pilard, François-Yves Dupradeau
Physical Chemistry Chemical Physics (2011) <https://doi.org/cv3hss>
DOI: [10.1039/c1cp20854c](https://doi.org/10.1039/c1cp20854c) · PMID: [21792425](#)

51. Validation and Comparison of Force Fields for Native Cyclodextrins in Aqueous Solution

Julia Gebhardt, Catharina Kleist, Sven Jakobtorweihen, Niels Hansen
The Journal of Physical Chemistry B (2018-01-24) <https://doi.org/gcv3xq>
DOI: [10.1021/acs.jpcb.7b11808](https://doi.org/10.1021/acs.jpcb.7b11808) · PMID: [29287148](#)

Supporting Information

A



B

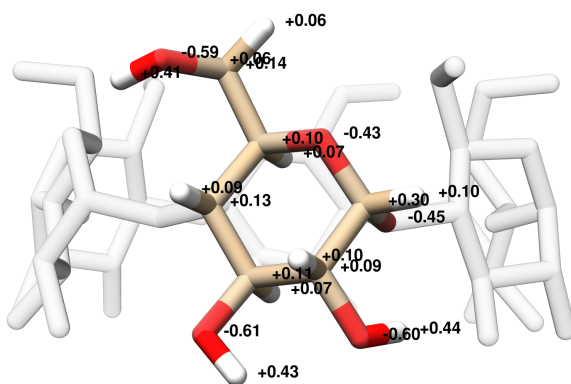
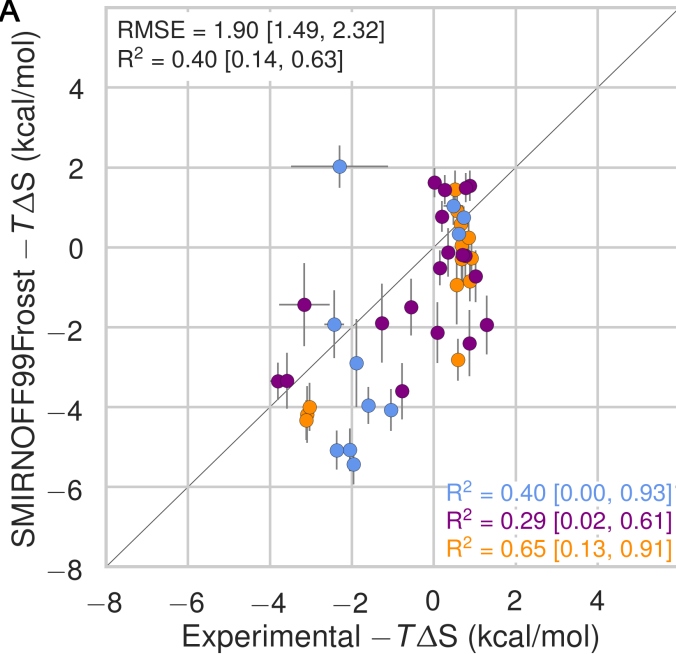
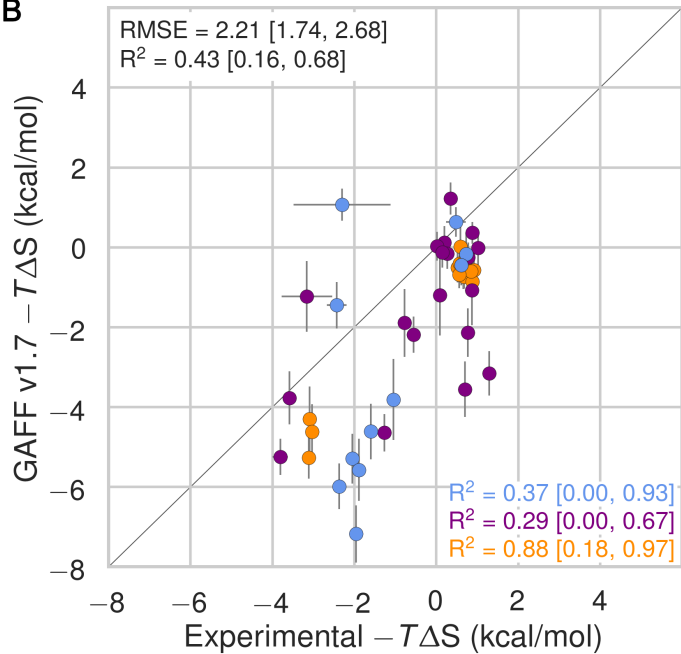


Figure 16: Comparison of AM1-BCC partial atomic charges assigned by running `antechamber` on a single glucose monomer (A) or on an entire α CD molecule (B) with the option `-pl 10` to specify the maximum path length used to determine the equivalence of atomic charges.

A



B



C

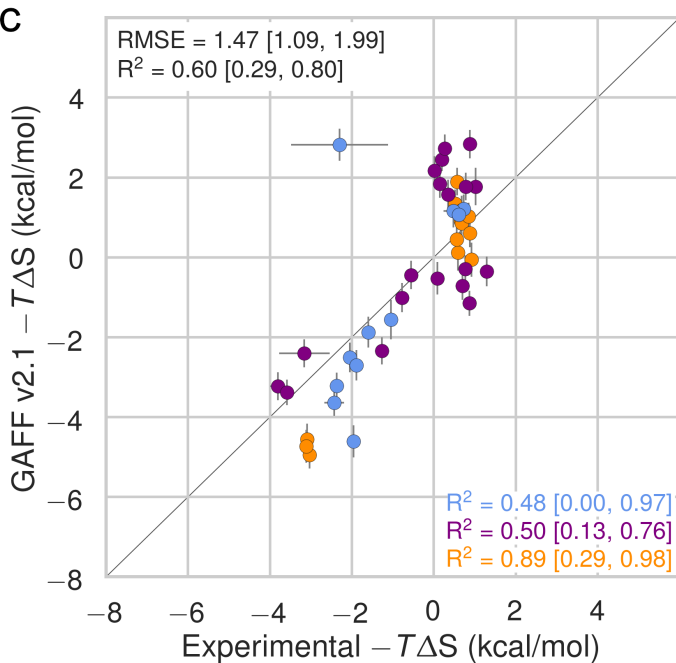


Figure 17: Comparison of calculated absolute binding entropies ($-T\Delta S$) with experiment with SMIRNOFF99Frosst parameters (top), GAFF v1.7 parameters (middle), or GAFF v2.1 parameters (bottom) applied to both host and guest. The orange, blue, and purple coloring distinguish the functional group of the guest as an ammonium, alcohol, or carboxylate, respectively.

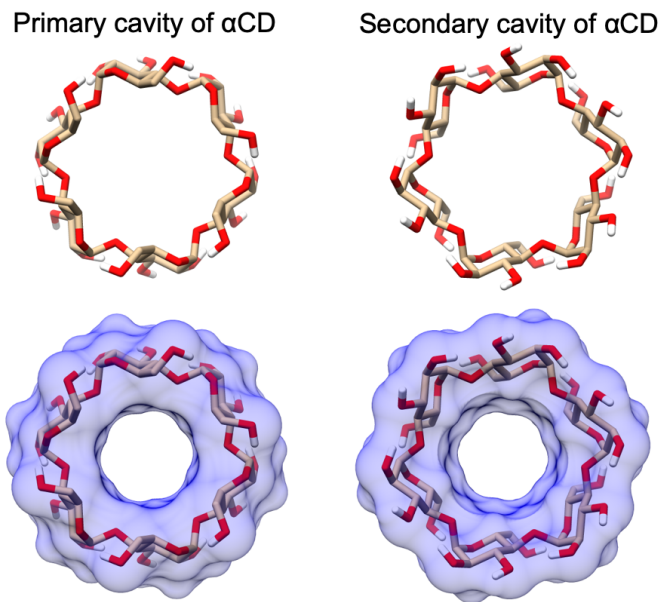


Figure 18: The primary (left) and secondary (right) cavity of α CD.

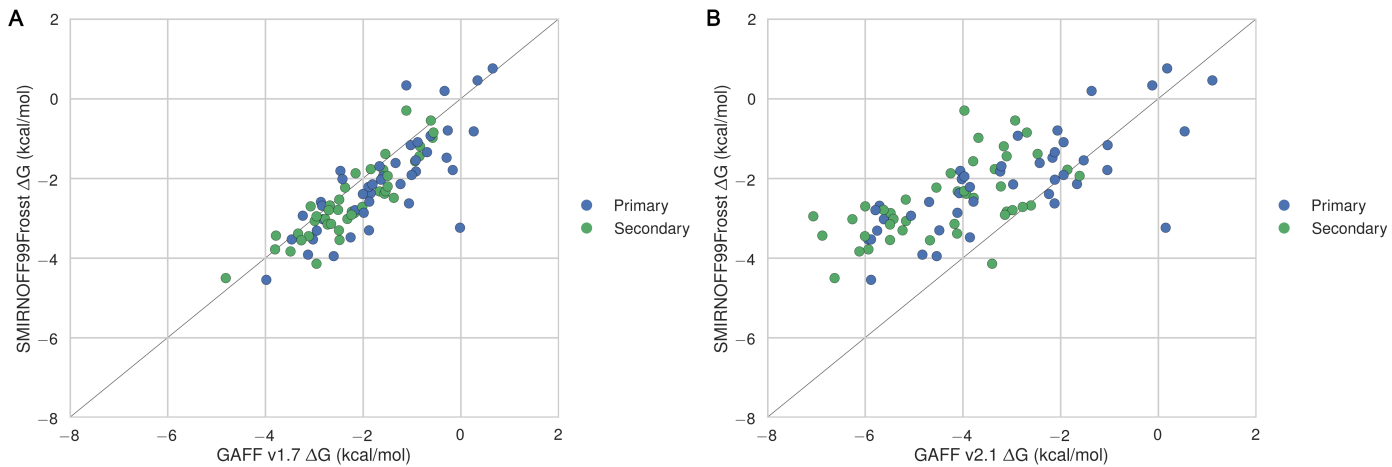


Figure 19: Binding free energies (ΔG) with the primary orientation results colored in blue and secondary orientation results colored in green.

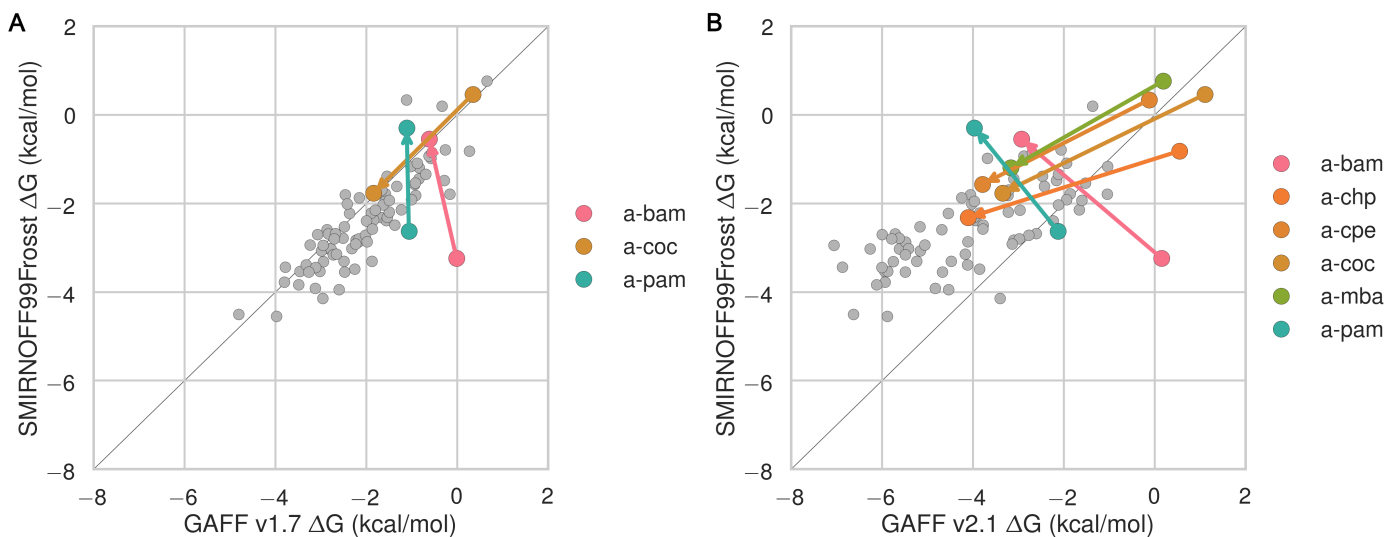


Figure 20: Binding free energies (ΔG) replotted from Figure 19 with points whose difference in binding free energy along either axis is greater than 2 kcal/mol shown in color. Arrows point from primary to secondary. **The arrow direction should match Figure 4, but it doesn't.**

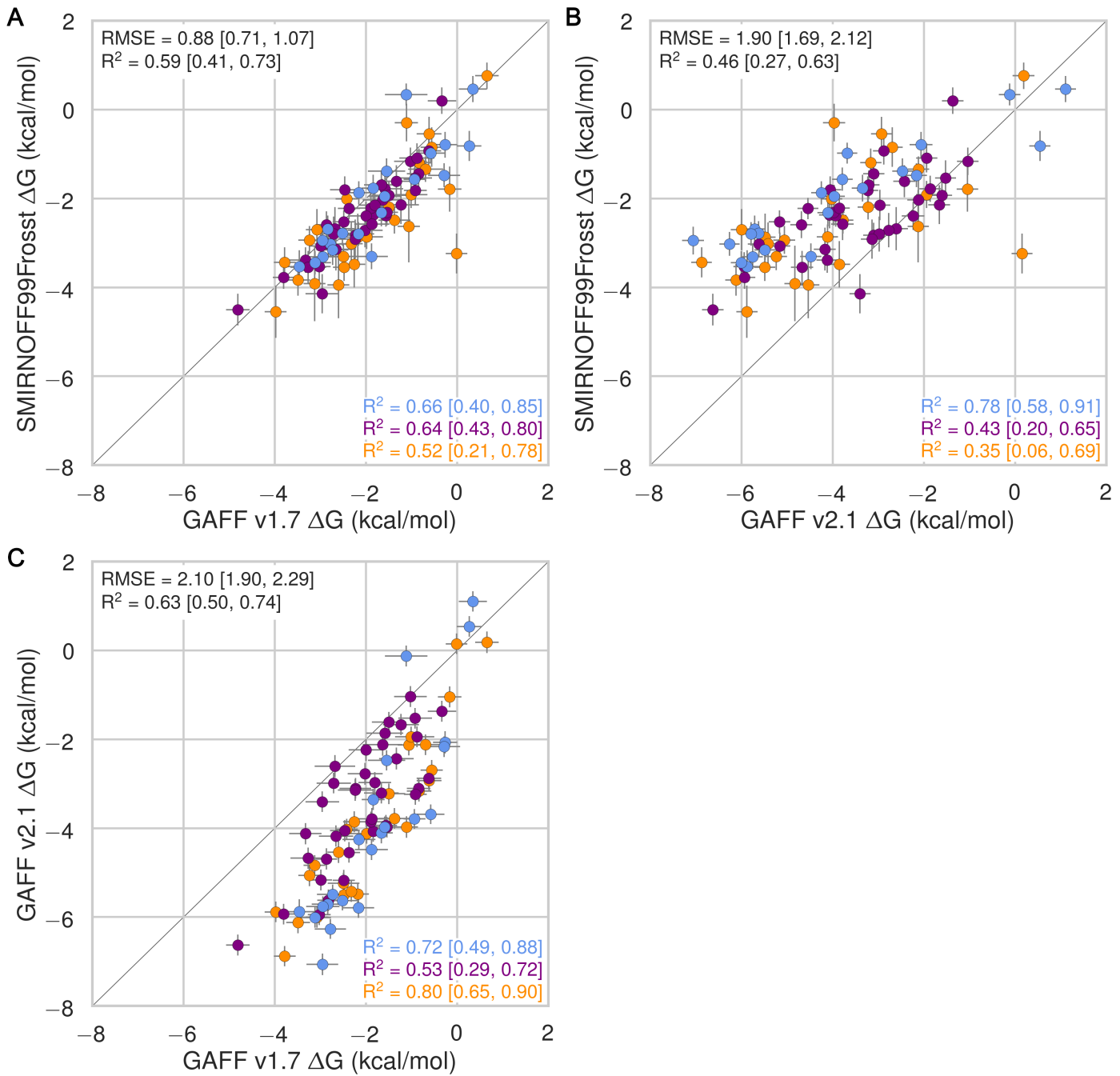


Figure 21: Comparison of calculated absolute binding free energies (ΔG) between force field combinations. The orange, blue, and purple coloring distinguish the functional group of the guest as an ammonium, alcohol, or carboxylate, respectively.

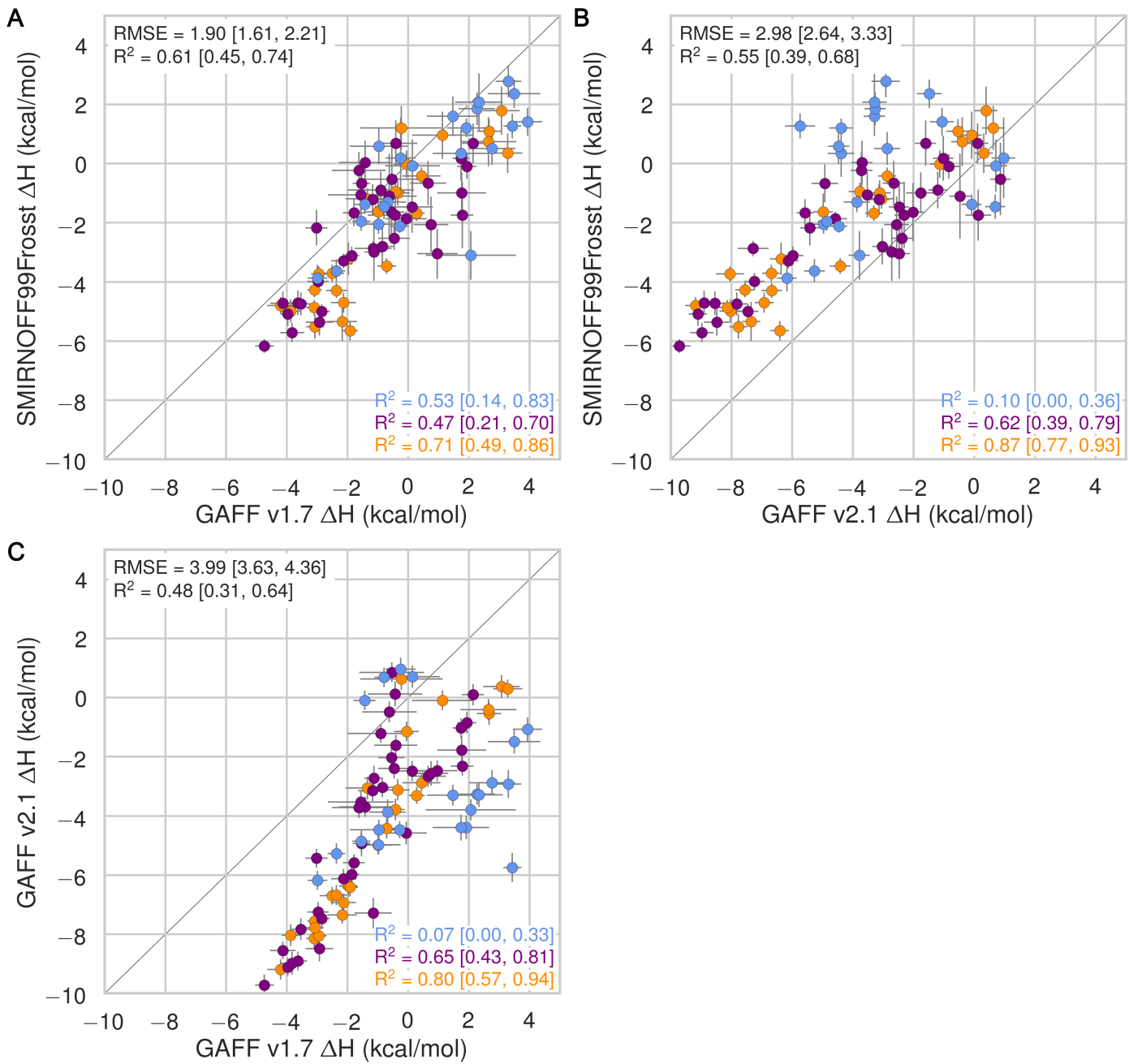


Figure 22: Comparison of calculated absolute binding free enthalpies (ΔH) between force field combinations. The orange, blue, and purple coloring distinguish the functional group of the guest as an ammonium, alcohol, or carboxylate, respectively.

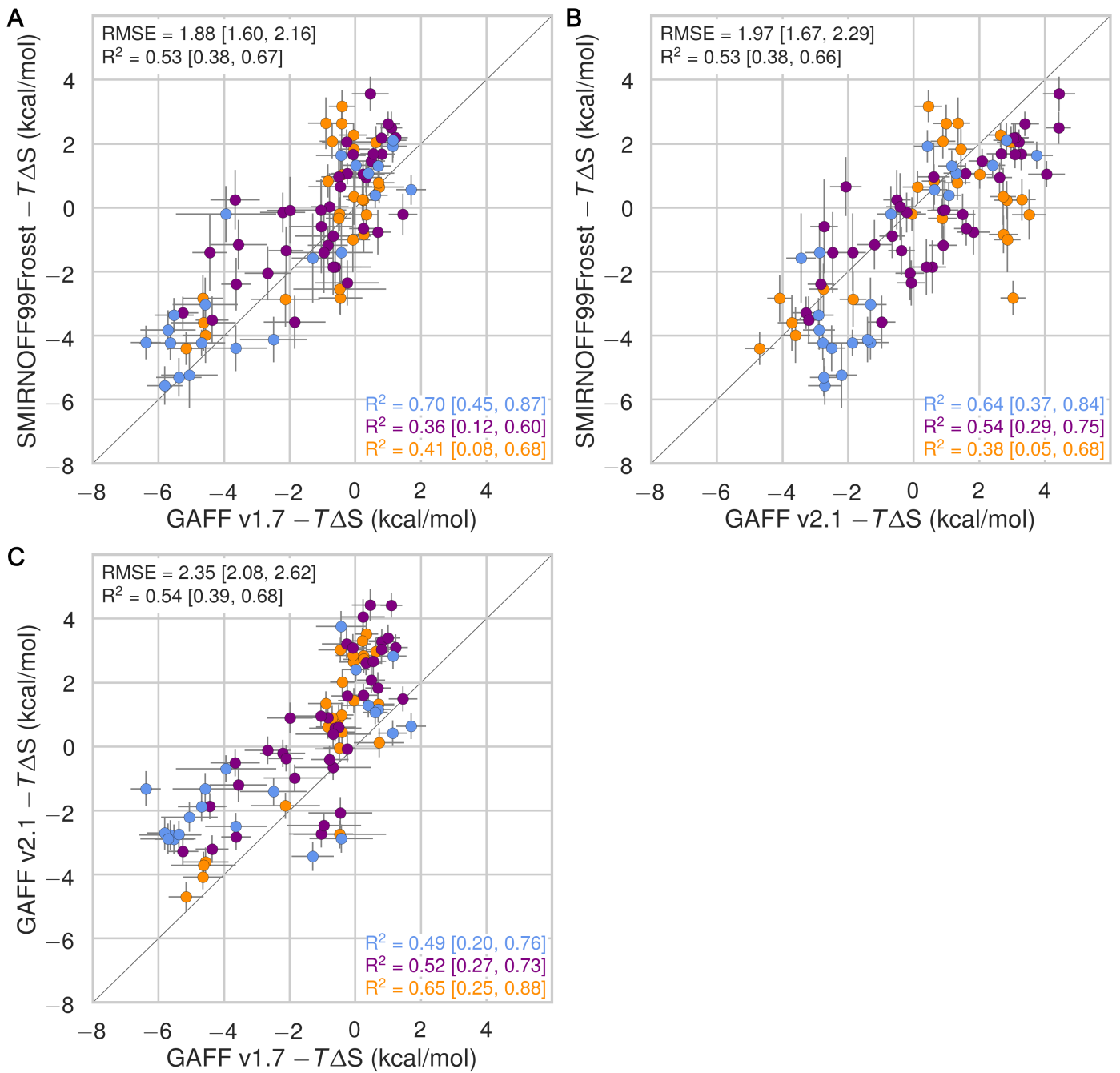


Figure 23: Comparison of calculated absolute binding free entropies ($-T\Delta S$) between force field combinations. The orange, blue, and purple coloring distinguish the functional group of the guest as an ammonium, alcohol, or carboxylate, respectively.

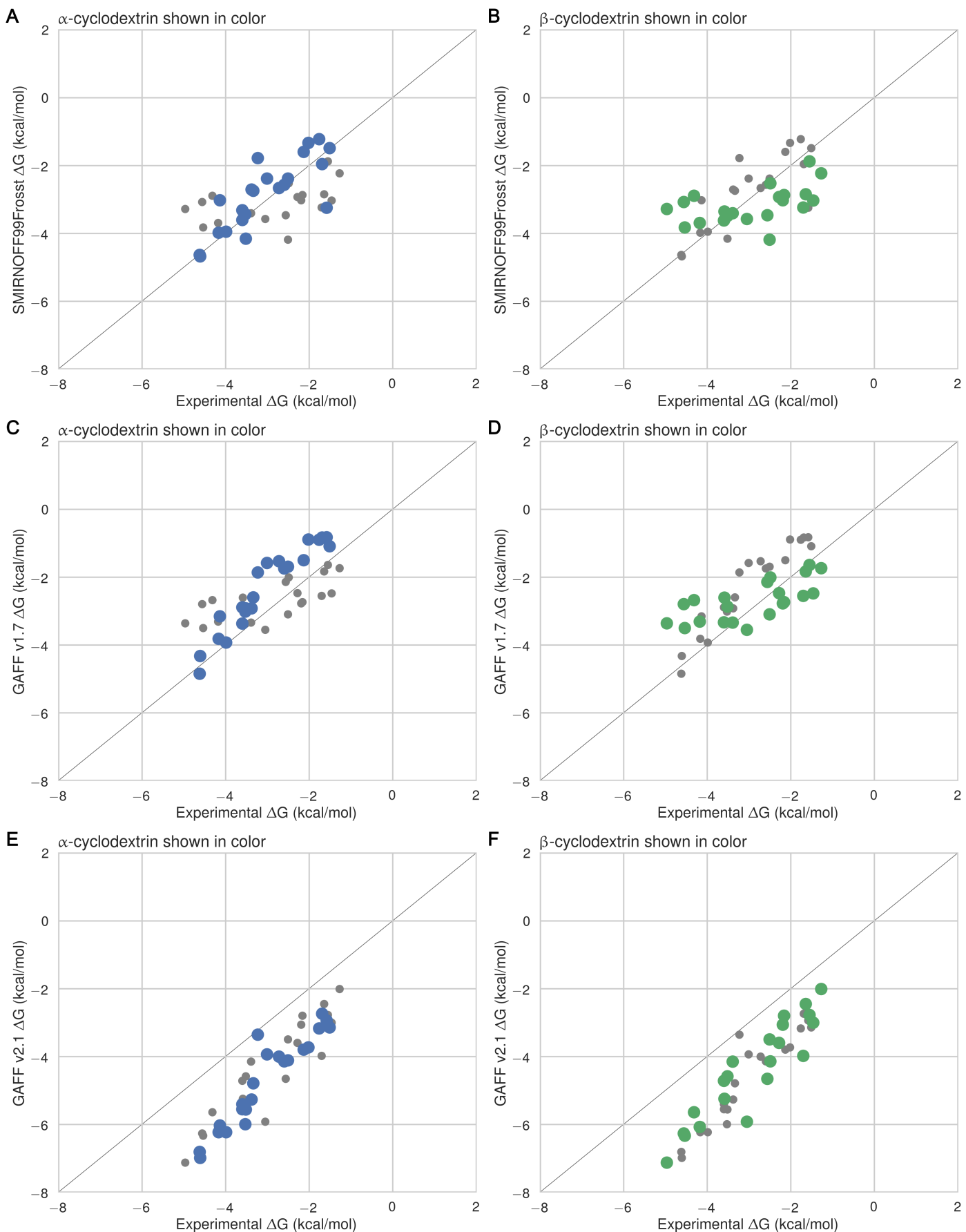


Figure 24: Binding free energies (ΔG) replotted from Figure 3, with α CD points colored in blue and β CD points in grey (left) or α CD points in grey with β CD points colored in green (right).

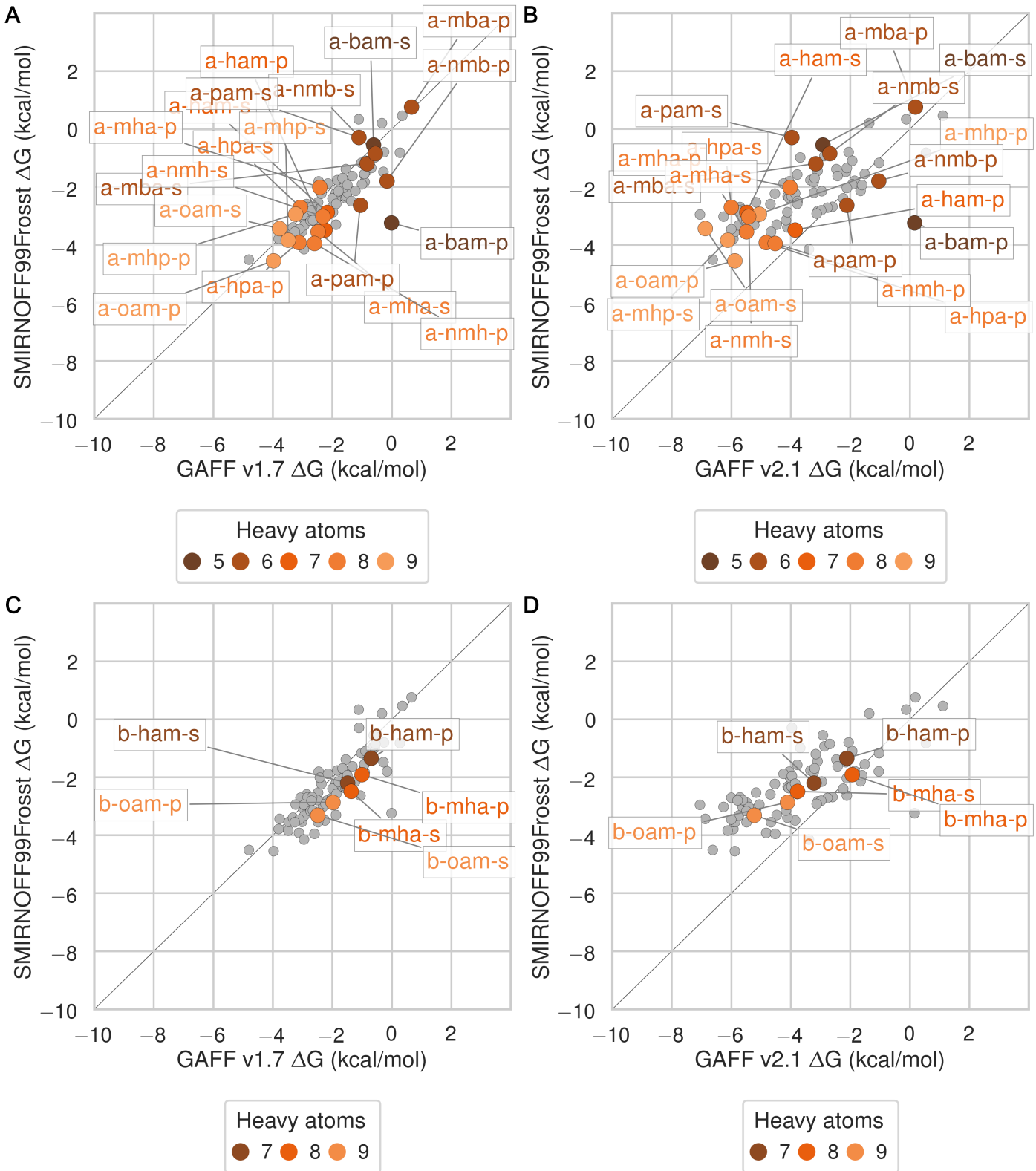


Figure 25: Binding free energy (ΔG) comparisons showing ammonium guests in color and highlighted.

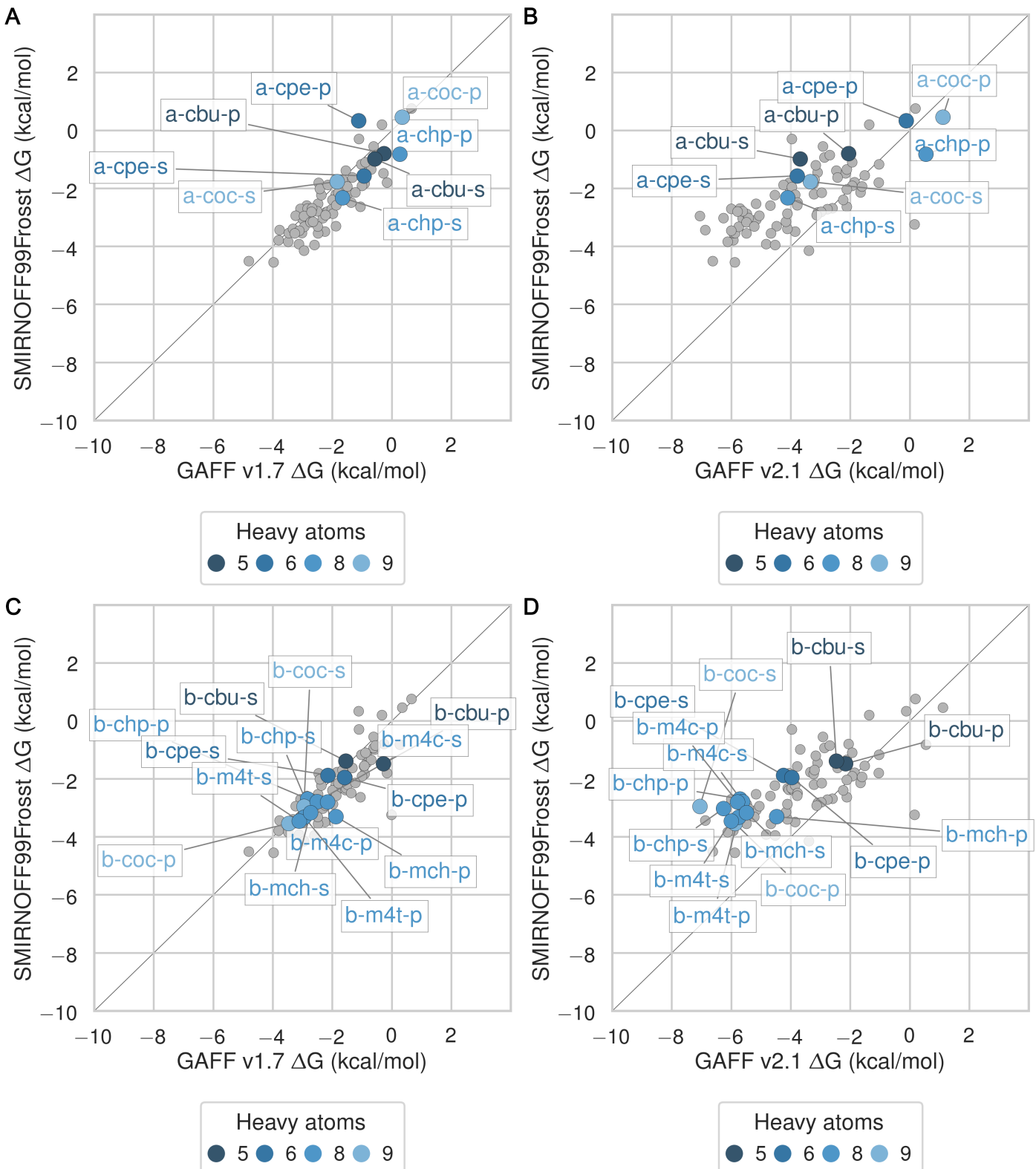


Figure 26: Binding free energy (ΔG) comparisons showing alcohols guests in color and highlighted.

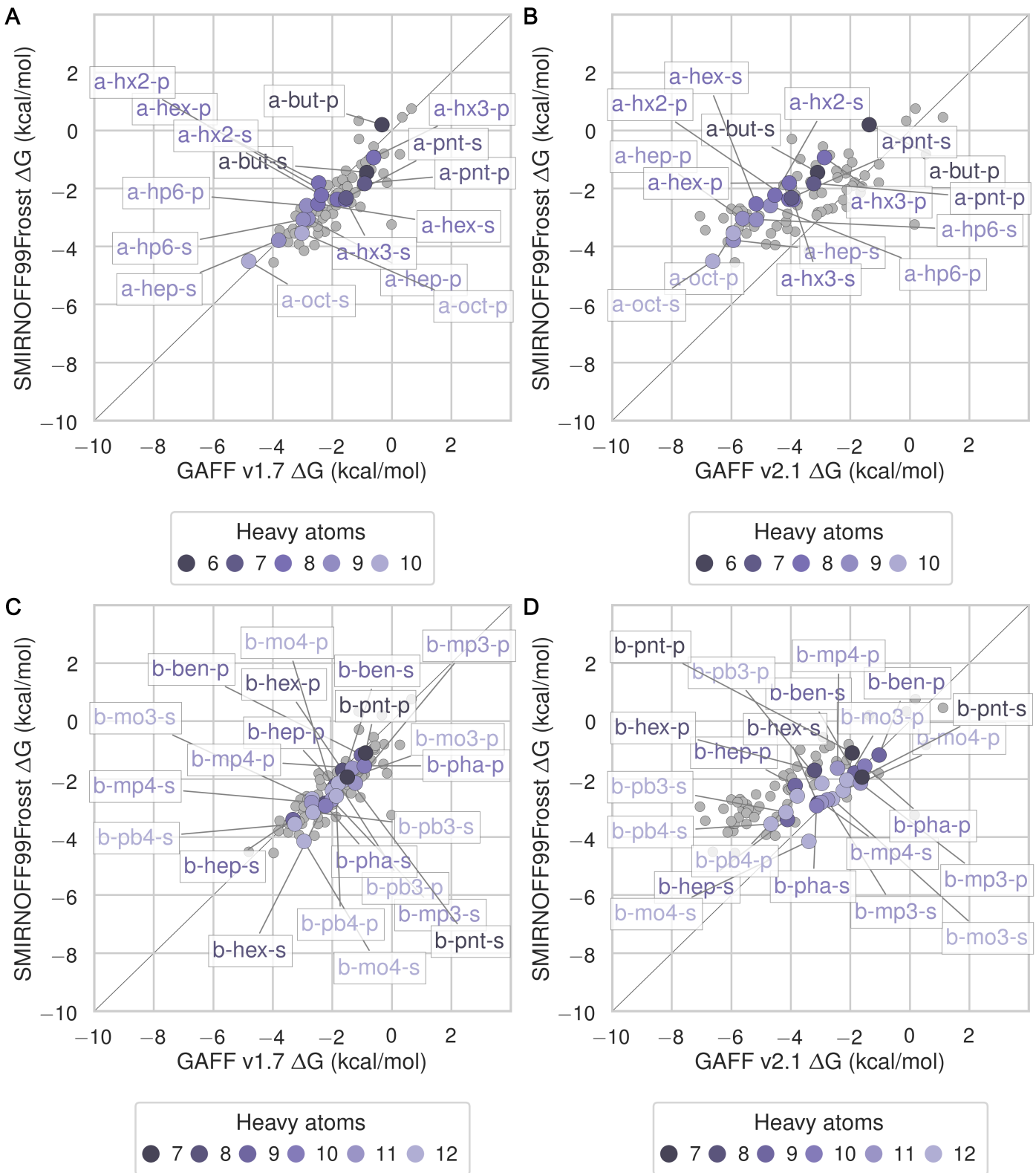


Figure 27: Binding free energy (ΔG) comparisons showing carboxylates guests in color and highlighted.

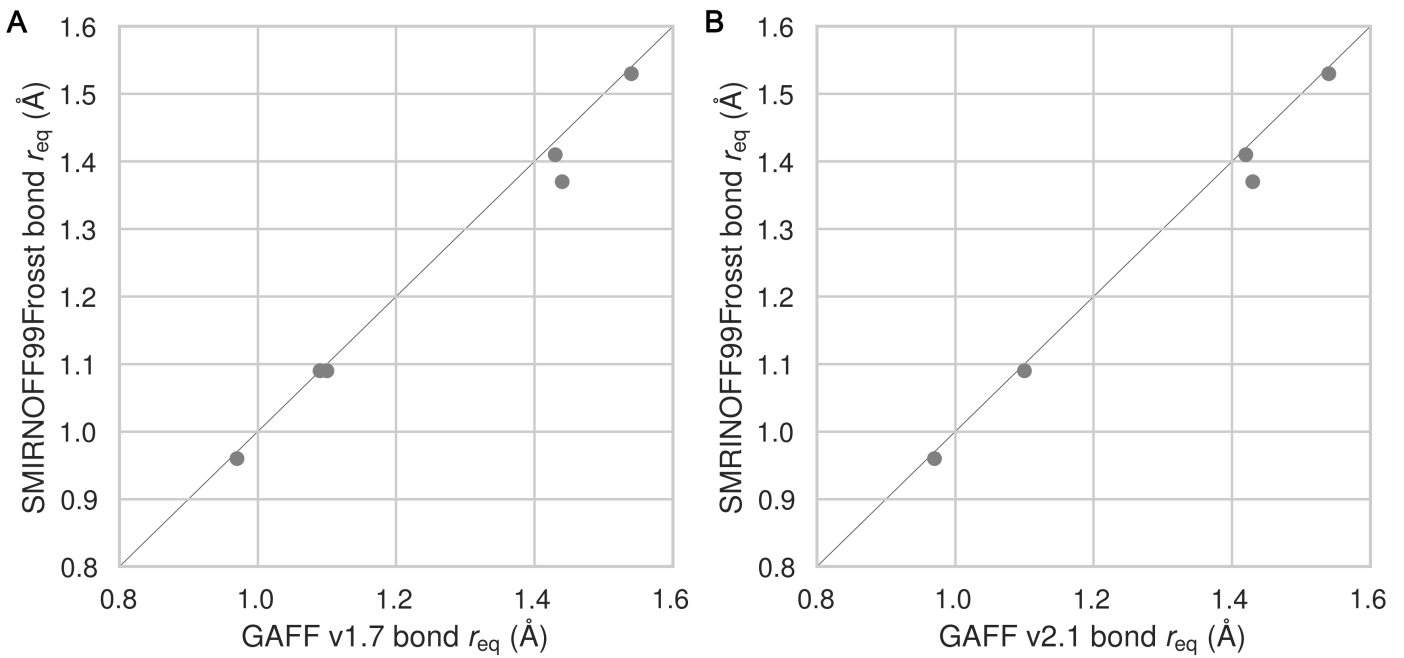


Figure 28: A comparison of bond equilibrium lengths for SMIRNOFF99Frosst, GAFF v1.7, and GAFF v2.1. Atom names refer to Figure 2.

Table 5: Experimental and predicted binding free energies (ΔG).

System	Experimental		SMIRNOFF99Frosst		GAFF v1.7		GAFF v2.1	
	Mean	SEM	Mean	SEM	Mean	SEM	Mean	SEM
a-bam	-1.58	0.02	-3.25	0.44	-0.82	0.21	-2.93	0.23
a-but	-1.51	0.04	-1.49	0.27	-1.09	0.20	-3.14	0.22
a-cbu	-2.02	0.02	-1.33	0.19	-0.89	0.22	-3.73	0.21
a-chp	-2.51	0.06	-2.38	0.28	-1.69	0.24	-4.11	0.23
a-coc	-3.23	1.14	-1.78	0.29	-1.86	0.24	-3.35	0.24
a-cpe	-2.13	0.02	-1.59	0.25	-1.50	0.29	-3.79	0.22
a-ham	-3.53	0.00	-3.43	0.30	-3.02	0.19	-5.99	0.17
a-hep	-3.99	0.01	-3.95	0.21	-3.93	0.20	-6.23	0.17
a-hex	-3.38	0.01	-2.70	0.21	-2.92	0.21	-5.27	0.20
a-hp6	-3.60	0.00	-3.32	0.23	-3.37	0.18	-5.41	0.18
a-hpa	-4.14	0.00	-3.02	0.32	-3.16	0.22	-6.03	0.22
a-hx2	-3.34	0.01	-2.74	0.20	-2.60	0.19	-4.79	0.18
a-hx3	-3.01	0.01	-2.39	0.25	-1.58	0.23	-3.94	0.23
a-mba	-1.76	0.02	-1.22	0.30	-0.89	0.25	-3.17	0.23
a-mha	-3.60	0.00	-3.60	0.29	-2.89	0.17	-5.55	0.22
a-mhp	-4.17	0.00	-3.98	0.29	-3.82	0.19	-6.23	0.21
a-nmb	-1.69	0.02	-1.95	0.42	-0.83	0.18	-2.74	0.21
a-nmh	-3.52	0.01	-4.15	0.59	-2.92	0.18	-5.56	0.19
a-oam	-4.61	0.01	-4.68	0.49	-4.33	0.17	-6.99	0.19
a-oct	-4.62	0.02	-4.64	0.30	-4.85	0.24	-6.81	0.19
a-pam	-2.72	0.00	-2.66	0.77	-1.53	0.18	-4.00	0.23
a-pnt	-2.60	0.01	-2.56	0.23	-1.74	0.19	-4.14	0.19

System	Experimental		SMIRNOFF99Frosst		GAFF v1.7		GAFF v2.1	
b-ben	-1.64	0.02	-2.85	0.62	-1.83	0.29	-2.45	0.17
b-cbu	-1.55	0.17	-1.88	0.20	-1.64	0.36	-2.77	0.17
b-chp	-4.56	0.01	-3.08	0.25	-2.79	0.34	-6.27	0.23
b-coc	-4.97	0.04	-3.28	0.23	-3.36	0.26	-7.13	0.22
b-cpe	-3.05	0.01	-3.57	0.34	-3.55	0.31	-5.93	0.27
b-ham	-2.49	0.08	-2.52	0.20	-2.01	0.26	-4.14	0.19
b-hep	-3.39	0.18	-3.41	0.28	-3.34	0.35	-4.15	0.23
b-hex	-2.28	0.03	-2.93	0.25	-2.47	0.27	-3.59	0.17
b-m4c	-4.32	0.01	-2.89	0.24	-2.68	0.29	-5.64	0.22
b-m4t	-4.54	0.01	-3.82	0.19	-3.50	0.26	-6.33	0.17
b-mch	-4.18	0.01	-3.69	0.22	-3.31	0.26	-6.07	0.17
b-mha	-2.56	0.07	-3.46	0.24	-2.14	0.28	-4.66	0.18
b-mo3	-2.16	0.01	-2.87	0.38	-2.73	0.41	-2.79	0.20
b-mo4	-2.51	0.01	-4.19	0.41	-3.10	0.31	-3.49	0.21
b-mp3	-1.46	0.04	-3.03	0.27	-2.48	0.28	-3.00	0.19
b-mp4	-2.19	0.01	-3.02	0.32	-2.77	0.34	-3.06	0.21
b-oam	-3.59	0.12	-3.35	0.28	-2.60	0.30	-5.25	0.23
b-pb3	-3.52	0.01	-3.49	0.32	-2.87	0.30	-4.58	0.17
b-pb4	-3.60	0.02	-3.62	0.33	-3.34	0.35	-4.71	0.23
b-pha	-1.70	0.05	-3.24	0.31	-2.55	0.29	-3.98	0.19
b-pnt	-1.27	0.32	-2.22	0.25	-1.73	0.29	-2.00	0.16

Table 6: Experimental and predicted binding enthalpies (ΔH).

System	Experimental		SMIRNOFF99Frosst		GAFF v1.7		GAFF v2.1	
	Mean	SEM	Mean	SEM	Mean	SEM	Mean	SEM
a-bam	-2.17	0.05	-0.43	0.28	-0.84	0.59	-3.05	0.38
a-but	-2.53	0.12	-0.76	0.59	-1.08	0.37	-4.91	0.42
a-cbu	-2.75	0.05	-2.08	0.21	-0.71	0.49	-4.94	0.29
a-chp	-2.99	0.23	-3.42	0.39	-2.33	0.28	-5.27	0.35
a-coc	-0.93	0.32	-3.80	0.45	-2.93	0.32	-6.17	0.32
a-cpe	-2.74	0.02	-1.93	0.30	-1.06	0.42	-4.86	0.29
a-ham	-4.19	0.02	-4.02	0.33	-2.33	0.30	-6.91	0.29
a-hep	-4.19	0.09	-4.72	0.33	-4.05	0.36	-8.68	0.24
a-hex	-3.40	0.02	-4.33	0.30	-2.95	0.30	-7.43	0.31
a-hp6	-4.48	0.02	-4.86	0.31	-3.73	0.21	-8.24	0.31
a-hpa	-4.66	0.02	-4.47	0.36	-2.65	0.30	-7.38	0.26
a-hx2	-4.12	0.06	-4.24	0.31	-2.35	0.32	-6.56	0.30
a-hx3	-3.36	0.05	-2.25	0.55	-2.80	0.32	-5.51	0.28
a-mba	-2.68	0.07	-0.95	0.41	-0.32	0.37	-3.11	0.36
a-mha	-4.28	0.02	-3.31	0.50	-2.16	0.25	-6.40	0.34

System	Experimental		SMIRNOFF99Frosst		GAFF v1.7		GAFF v2.1	
a-mhp	-4.74	0.02	-4.89	0.23	-3.41	0.23	-8.12	0.28
a-nmb	-2.57	0.06	-1.10	0.28	0.03	0.23	-3.34	0.27
a-nmh	-4.20	0.08	-4.20	0.48	-2.54	0.24	-6.74	0.30
a-oam	-5.46	0.03	-4.93	0.28	-3.73	0.33	-8.02	0.28
a-oct	-4.89	0.03	-6.08	0.21	-4.69	0.29	-9.53	0.30
a-pam	-3.28	0.02	-1.72	0.61	-0.84	0.28	-4.45	0.33
a-pnt	-2.75	0.01	-2.05	0.37	-1.62	0.33	-5.99	0.30
b-ben	-2.51	0.08	-0.45	0.56	-0.76	0.82	-1.30	0.26
b-cbu	0.88	0.17	0.05	0.83	-0.19	0.46	0.87	0.29
b-chp	-2.96	0.01	0.88	0.40	1.82	0.61	-4.39	0.31
b-coc	-3.92	0.06	0.80	0.47	0.45	0.98	-5.57	0.44
b-cpe	-1.09	0.01	1.86	0.37	3.62	0.65	-1.32	0.30
b-ham	0.60	0.05	1.66	0.68	2.29	0.78	0.42	0.33
b-hep	0.42	0.04	-0.05	0.38	1.91	0.29	-0.92	0.27
b-hex	1.31	0.04	0.41	0.65	1.30	0.60	-0.21	0.27
b-m4c	-2.27	0.01	2.18	0.48	2.62	0.55	-3.13	0.30
b-m4t	-2.17	0.02	1.26	0.45	2.49	0.51	-3.11	0.29
b-mch	-2.29	0.03	-0.79	1.08	2.27	0.73	-3.37	0.34
b-mha	0.47	0.03	0.53	0.55	2.48	0.64	0.28	0.29
b-mo3	-2.93	0.03	-2.66	0.46	-0.59	0.45	-2.50	0.28
b-mo4	-1.96	0.01	-2.69	0.58	-0.91	0.33	-3.05	0.29
b-mp3	-2.75	0.13	-1.09	0.68	0.68	0.48	-2.64	0.31
b-mp4	-2.89	0.05	-2.84	0.76	0.78	0.60	-2.34	0.28
b-oam	-0.48	0.03	0.98	0.41	2.66	0.43	-0.52	0.34
b-pb3	-2.25	0.01	-1.59	0.94	1.78	0.36	-2.24	0.30
b-pb4	-2.82	0.01	-0.02	0.62	-1.44	0.78	-3.70	0.29
b-pha	-1.79	0.11	-1.10	0.69	-1.34	0.97	-3.45	0.36
b-pnt	1.89	0.53	-0.79	1.01	-0.51	0.84	0.40	0.31

Table 7: Experimental and predicted binding entropies ($-T\Delta S$).

System	Experimental		SMIRNOFF99Frosst		GAFF v1.7		GAFF v2.1	
	Mean	SEM	Mean	SEM	Mean	SEM	Mean	SEM
a-bam	0.59	0.05	-2.82	0.53	0.02	0.63	0.11	0.45
a-but	1.02	0.13	-0.73	0.65	-0.01	0.42	1.77	0.47
a-cbu	0.73	0.05	0.75	0.28	-0.17	0.54	1.21	0.36
a-chp	0.48	0.24	1.04	0.48	0.63	0.37	1.16	0.41
a-coc	-2.30	1.18	2.02	0.53	1.07	0.40	2.82	0.40
a-cpe	0.61	0.03	0.33	0.39	-0.44	0.51	1.07	0.37
a-ham	0.66	0.02	0.59	0.44	-0.68	0.36	0.92	0.34
a-hep	0.20	0.09	0.77	0.39	0.12	0.41	2.45	0.29

System	Experimental		SMIRNOFF99Frosst		GAFF v1.7		GAFF v2.1	
a-hex	0.02	0.02	1.62	0.37	0.03	0.36	2.17	0.37
a-hp6	0.88	0.02	1.54	0.38	0.37	0.27	2.84	0.36
a-hpa	0.52	0.02	1.45	0.48	-0.50	0.37	1.35	0.34
a-hx2	0.78	0.06	1.49	0.37	-0.25	0.37	1.77	0.35
a-hx3	0.35	0.05	-0.13	0.61	1.23	0.40	1.58	0.36
a-mba	0.92	0.07	-0.27	0.51	-0.57	0.44	-0.06	0.43
a-mha	0.68	0.02	-0.29	0.58	-0.73	0.30	0.85	0.40
a-mhp	0.57	0.02	0.92	0.37	-0.41	0.30	1.89	0.35
a-nmb	0.88	0.06	-0.85	0.50	-0.86	0.29	0.61	0.35
a-nmh	0.68	0.08	0.05	0.76	-0.38	0.30	1.18	0.36
a-oam	0.85	0.03	0.25	0.57	-0.60	0.37	1.02	0.34
a-oct	0.27	0.04	1.44	0.37	-0.16	0.38	2.72	0.36
a-pam	0.56	0.02	-0.94	0.98	-0.68	0.34	0.45	0.40
a-pnt	0.15	0.01	-0.51	0.43	-0.12	0.38	1.84	0.36
b-ben	0.87	0.08	-2.40	0.83	-1.07	0.87	-1.15	0.31
b-cbu	-2.43	0.24	-1.93	0.85	-1.45	0.58	-3.64	0.34
b-chp	-1.60	0.01	-3.96	0.47	-4.61	0.69	-1.87	0.39
b-coc	-1.05	0.07	-4.08	0.53	-3.81	1.02	-1.56	0.49
b-cpe	-1.96	0.01	-5.43	0.51	-7.17	0.72	-4.60	0.40
b-ham	-3.09	0.09	-4.19	0.71	-4.29	0.82	-4.56	0.38
b-hep	-3.81	0.18	-3.36	0.47	-5.25	0.45	-3.23	0.35
b-hex	-3.59	0.05	-3.34	0.70	-3.77	0.66	-3.38	0.32
b-m4c	-2.05	0.01	-5.07	0.54	-5.29	0.62	-2.51	0.37
b-m4t	-2.37	0.02	-5.08	0.49	-5.99	0.57	-3.22	0.33
b-mch	-1.89	0.03	-2.90	1.10	-5.58	0.78	-2.70	0.38
b-mha	-3.03	0.08	-4.00	0.60	-4.62	0.69	-4.94	0.34
b-mo3	0.77	0.03	-0.20	0.60	-2.14	0.61	-0.29	0.34
b-mo4	-0.55	0.01	-1.50	0.71	-2.19	0.46	-0.45	0.36
b-mp3	1.29	0.14	-1.94	0.74	-3.16	0.56	-0.35	0.37
b-mp4	0.70	0.05	-0.19	0.83	-3.55	0.69	-0.72	0.35
b-oam	-3.11	0.12	-4.33	0.50	-5.26	0.53	-4.73	0.41
b-pb3	-1.27	0.01	-1.90	0.99	-4.64	0.47	-2.34	0.34
b-pb4	-0.78	0.02	-3.60	0.71	-1.90	0.85	-1.01	0.37
b-phä	0.09	0.12	-2.14	0.76	-1.21	1.01	-0.52	0.41
b-pnt	-3.16	0.62	-1.43	1.04	-1.22	0.89	-2.40	0.35

Table 8: Predicted thermodynamic properties for each force field relative to experiment on ammonium guests.

		RMSE		MSE		R ²		Slope		Intercept	
ΔG	SMIRNO FF99Frosst	0.76	[0.43, 1.11]	-0.10	[-0.54, 0.31]	0.48	[0.07, 0.84]	0.69	[0.19, 1.16]	-1.06	[0.54, -2.77]

		RMSE		MSE		R²		Slope		Intercept	
ΔG	GAFF v1.7	0.77	[0.59, 0.95]	0.69	[0.51, 0.88]	0.90	[0.76, 0.98]	1.08	[0.88, 1.26]	0.95	[1.56, 0.32]
ΔG	GAFF v2.1	1.85	[1.59, 2.09]	-1.79	[-2.04, -1.53]	0.93	[0.83, 0.98]	1.32	[1.13, 1.51]	-0.80	[-0.20, -1.46]
ΔH	SMIRNO FF99Frost	1.15	[0.77, 1.51]	0.83	[0.39, 1.27]	0.89	[0.76, 0.97]	1.15	[0.89, 1.53]	1.31	[2.81, 0.38]
ΔH	GAFF v1.7	2.12	[1.77, 2.47]	2.02	[1.67, 2.37]	0.92	[0.80, 0.98]	1.09	[0.86, 1.35]	2.29	[3.34, 1.39]
ΔH	GAFF v2.1	1.90	[1.31, 2.43]	-1.51	[-2.15, -0.88]	0.96	[0.91, 0.99]	1.54	[1.38, 1.83]	0.09	[1.18, -0.44]
-TΔS	SMIRNO FF99Frost	1.47	[0.90, 2.10]	-0.93	[-1.59, -0.31]	0.65	[0.13, 0.91]	0.99	[0.58, 1.35]	-0.88	[-0.09, -1.66]
-TΔS	GAFF v1.7	1.45	[1.14, 1.79]	-1.33	[-1.66, -1.00]	0.88	[0.18, 0.97]	1.04	[-0.02, 1.37]	-1.27	[-0.55, -1.62]
-TΔS	GAFF v2.1	1.04	[0.67, 1.40]	-0.27	[-0.84, 0.26]	0.89	[0.29, 0.98]	1.36	[-0.53, 1.66]	-0.12	[1.16, -0.59]

Table 9: Predicted thermodynamic properties for each force field relative to experiment on carboxylate guests.

		RMSE		MSE		R²		Slope		Intercept	
ΔG	SMIRNO FF99Frost	0.87	[0.59, 1.16]	-0.36	[-0.74, -0.01]	0.34	[0.02, 0.68]	0.45	[0.11, 0.75]	-1.85	[-0.91, -2.83]
ΔG	GAFF v1.7	0.68	[0.49, 0.88]	0.03	[-0.28, 0.34]	0.52	[0.16, 0.80]	0.68	[0.33, 0.97]	-0.84	[0.08, -1.75]
ΔG	GAFF v2.1	1.46	[1.21, 1.71]	-1.36	[-1.61, -1.10]	0.81	[0.61, 0.93]	1.18	[0.85, 1.46]	-0.87	[0.02, -1.74]
ΔH	SMIRNO FF99Frost	1.41	[0.94, 1.93]	0.20	[-0.43, 0.84]	0.53	[0.20, 0.79]	0.83	[0.40, 1.53]	-0.14	[2.12, -1.30]
ΔH	GAFF v1.7	1.95	[1.34, 2.55]	1.24	[0.55, 1.93]	0.47	[0.13, 0.78]	0.79	[0.32, 1.49]	0.82	[3.10, -0.54]
ΔH	GAFF v2.1	2.43	[1.75, 3.06]	-1.73	[-2.51, -0.96]	0.69	[0.49, 0.85]	1.40	[0.99, 2.29]	-0.66	[2.15, -1.61]
-TΔS	SMIRNO FF99Frost	1.73	[1.17, 2.29]	-0.57	[-1.32, 0.16]	0.29	[0.02, 0.61]	0.62	[0.16, 1.09]	-0.68	[0.05, -1.43]
-TΔS	GAFF v1.7	2.07	[1.35, 2.76]	-1.22	[-2.00, -0.46]	0.29	[0.00, 0.67]	0.63	[-0.02, 1.18]	-1.31	[-0.58, -2.09]
-TΔS	GAFF v2.1	1.46	[1.12, 1.77]	0.37	[-0.27, 1.00]	0.50	[0.13, 0.76]	0.93	[0.58, 1.30]	0.37	[1.07, -0.34]

Table 10: Predicted thermodynamic properties for each force field relative to experiment on cyclic alcohol guests.

		RMSE		MSE		R²		Slope		Intercept	
ΔG	SMIRNO FF99Frost	1.07	[0.66, 1.58]	0.71	[0.22, 1.21]	0.54	[0.09, 0.86]	0.55	[0.20, 0.84]	-0.84	[0.16, -2.09]
ΔG	GAFF v1.7	1.22	[0.86, 1.67]	0.93	[0.45, 1.41]	0.56	[0.12, 0.89]	0.59	[0.25, 0.89]	-0.47	[0.64, -1.77]

		RMSE		MSE		R ²		Slope		Intercept	
ΔG	GAFF v2.1	1.80	[1.48, 2.15]	-1.64	[-2.04, -1.14]	0.73	[0.19, 0.98]	1.01	[0.49, 1.27]	-1.63	[-0.67, -3.19]
ΔH	SMIRNOFF99Frosst	2.88	[1.99, 3.68]	1.66	[0.21, 3.03]	0.09	[0.00, 0.44]	0.07	[-1.28, 1.67]	-0.29	[3.93, -4.06]
ΔH	GAFF v1.7	3.63	[2.67, 4.47]	2.66	[1.13, 4.07]	0.10	[0.00, 0.57]	0.12	[-1.09, 2.28]	0.91	[6.66, -2.47]
ΔH	GAFF v2.1	2.08	[1.18, 3.16]	-1.64	[-2.54, -0.91]	0.54	[0.00, 0.97]	1.08	[-0.37, 1.90]	-1.51	[0.83, -5.50]
-TΔS	SMIRNOFF99Frosst	2.47	[1.62, 3.36]	-0.96	[-2.22, 0.52]	0.40	[0.00, 0.93]	1.18	[-0.45, 2.26]	-0.88	[0.36, -3.60]
-TΔS	GAFF v1.7	3.00	[2.07, 3.88]	-1.73	[-3.14, -0.18]	0.37	[0.00, 0.93]	1.23	[-0.38, 2.48]	-1.59	[-0.31, -4.23]
-TΔS	GAFF v2.1	1.80	[0.68, 3.19]	-0.00	[-0.98, 1.27]	0.48	[0.00, 0.97]	1.13	[-0.22, 1.96]	0.08	[1.14, -1.79]

Table 11: Dihedral parameter differences between SMIRNOFF99Frosst and GAFF v1.7. Atom names refer to Figure 2.

						SMIRNOFF99Frosst	GAFF v1.7
Atom 1	Atom 2	Atom 3	Atom 4	Per	Phase	Height (kcal/mol)	
H1	C1	C2	O2	1	0	0.25	
H1	C1	C2	O2	3	0	0.00	
						0.16	

Table 12: Dihedral parameter differences between SMIRNOFF99Frosst and GAFF v2.1, where one dihedral has fewer or more periodicity terms than the corresponding term in the other force field. Atom names refer to 2.

						SMIRNOFF99Frosst	GAFF v2.1
Atom 1	Atom 2	Atom 3	Atom 4	Per	Phase	Height (kcal/mol)	
C1	C2	O2	HO2	1	0	0.25	
C1	C2	O2	HO2	3	0	0.16	
C1	O5	C5	C4	1	0	-	
C1	O5	C5	C4	2	0	0.10	
C1	O5	C5	C4	3	0	0.38	
C1	O5	C5	C6	1	0	-	
C1	O5	C5	C6	2	0	0.10	
C1	O5	C5	C6	3	0	0.38	
C2	C1	O5	C5	1	0	-	
C2	C1	O5	C5	2	0	0.10	
C2	C1	O5	C5	3	0	0.38	
C2	C3	O3	HO3	1	0	0.25	
C2	C3	O3	HO3	3	0	0.16	
C5	C6	O6	HO6	1	0	0.25	
C5	C6	O6	HO6	3	0	0.16	
H1	C1	C2	O2	1	0	0.25	
H1	C1	C2	O2	3	0	0.00	

						SMIRNOFF99Frosst	GAFF v2.1
O1	C1	C2	O2	1	0	–	0.02
O1	C1	C2	O2	2	0	1.18	0.00
O1	C1	C2	O2	3	0	0.14	1.01
O2	C2	C1	O5	1	0	–	0.02
O2	C2	C1	O5	2	0	1.18	0.00
O2	C2	C1	O5	3	0	0.14	1.01
O5	C5	C6	O6	1	0	–	0.02
O5	C5	C6	O6	2	0	1.18	0.00
O5	C5	C6	O6	3	0	0.14	1.01
HO2	O2	C2	C3	1	0	0.25	–
HO2	O2	C2	C3	3	0	0.16	0.00
HO3	O3	C3	C4	1	0	0.25	–
HO3	O3	C3	C4	3	0	0.16	0.00